

Novel Selective Inhibitors of the Zinc Plasmodial Aminopeptidase PfA-M1 as Potential Antimalarial Agents

Marion Flipo,[†] Terence Beghyn,[†] Virginie Leroux,[†] Isabelle Florent,[‡] Benoit P. Deprez,^{*,†} and Rebecca F. Deprez-Poulain[†]

Inserm, U761, Biostructures and Drug Discovery, Lille F-59006 France, Faculté de Pharmacie, Université de Lille2, Lille F-59006 France, Institut Pasteur de Lille, Lille F-59019 France, and USM504/EA3335 Muséum National d'Histoire Naturelle, Regulations, Development, Molecular diversity, Paris, F-75005 France

Received October 9, 2006

Proteases that are expressed during the erythrocytic stage of *Plasmodium falciparum* are newly explored drug targets for the treatment of malaria. We report here the discovery of potent inhibitors of PfA-M1, a metallo-aminopeptidase of the parasite. These compounds are based on a malonic hydroxamic template and present a very good selectivity toward neutral aminopeptidase (APN-CD13), a related protease in mammals. Structure–activity relationships in these series are described. Further optimization of the best inhibitor yielded a nanomolar, selective inhibitor of PfA-M1. This inhibitor displays good physicochemical and pharmacokinetic properties and a promising antimalarial activity.

Introduction

Malaria is a major disease in developing countries, causing every year 1–2 million deaths, a majority of cases being young children in Africa.¹ This burdensome disease is caused by protozoa parasites *Plasmodium*. The species *P. falciparum* is by itself responsible for the majority of deaths. The parasite is transmitted by the female *Anopheles* mosquito and transits through the liver and the blood of the mammalian host. The blood stages of the parasites are those that cause the symptoms. Apart from quinoline-based antimalarials, antifolates, and antibiotics, the endoperoxide artemisinin and its synthetic derivatives are widely used to combat the disease.² Unfortunately, there has been a spread of resistant strains of the parasite to the current therapeutics in numerous countries.^{3–4} This antimalarial drug resistance, which is also an economic burden to these countries, has become one of the greatest challenges in malaria control.⁵ There is, thus, a need for new therapies, which development can be accelerated by the recent publication of *Plasmodium* genome.^{6–8}

Targeting the erythrocytic stage of the parasite is widely investigated for the design of antimalarials.^{9–10} In this context, host hemoglobin degradation pathways are of high interest. They produce both heme, detoxified by the parasite as hemozoin (the malarial pigment), and globin, the source of amino acids for the parasite. This offers two possible strategies to combat the disease: (1) inhibition of heme detoxification, so that heme accumulates as its lethal form for the parasite and (2) inhibition of proteases responsible for globin digestion. Interestingly, some proteases are not only involved in globin hydrolysis, but also in parasite release and reinvasion of red blood cells.^{11–13} As a consequence of these important functions and the successful work done on proteases in other pathologies (Aids, hypertension), proteases expressed in the erythrocyte cycle of *Plasmodium* are now considered as promising molecular targets for drug discovery.^{12,14} So far, 92 proteases have been found in the genome of the parasite, including serine-, aspartyl-, cysteine-,

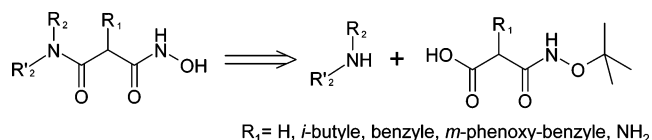


Figure 1. Markush formula of the library members.

and metallo-proteases, all of them being expressed at the erythrocytic stage.^{15–17}

At present, the protease inhibitors described are inhibitors of the two classes of acidic endopeptidases (plasmepsins and falcipains) that initiate the degradation of globin in the digestive vacuole. Hallberg et al. have developed potent and selective inhibitors of the aspartyl-proteases plasmepsin I, II, and IV, derived from an hydroxyethylene scaffold or a related transition state mimick.^{18–20} Inhibitors of the entire family of plasmepsins, including the related histoaspartyl-protease (HAP), have also been described.²¹ In parallel, HIV protease inhibitors have been shown to inhibit plasmepsin II and IV in the submicromolar range.²² The teams of Rosenthal and Avery have designed, or identified by virtual screening, irreversible or reversible inhibitors of falcipain-2 and -3.^{23–26} Greenbaum et al. designed thiosemicarbazones inhibitors of several parasitic falcipains including falcipain-2, and recently, Bogyo et al. designed electrophilic azapeptides as cysteine protease probes.^{27,28}

Among the metalloproteases of *Plasmodium*, both endo- and exo-peptidases have been described along with falcilysin, methionine aminopeptidase 1b, leucylaminopeptidase (LAP), and PfA-M1.^{29–32} Falcilysin is an endopeptidase with dual specificity. It is involved in the intravacuolar digestion of globin, in peptide degradation in apicoplast and has no reported inhibitor.^{29,33} Methionine aminopeptidase 1b has recently been screened for inhibitors.³² LAP is a tripeptide aminopeptidase of the M17-family.³⁰ PfA-M1 belongs to the M1 family and displays a strict aminopeptidase activity at pH 7.4 and a broad substrate spectrum.^{34,35} It is involved both in haemoglobin breakdown and erythrocyte reinvasion. Indeed, PfA-M1 localizes differently in trophozoites and schizonts, suggesting two different roles in critical steps of the intraerythrocytic life of the parasite.³⁵ (1) In the trophozoite, it accumulates at the cytoplasmic side of the digestive vacuole and could be involved in the cytoplasmic degradation of oligopeptides that are the end-

* To whom correspondence should be addressed. INSERM U761, Faculté de Pharmacie, 3 rue du Pr. Laguesse, F-59006 Lille Cedex, France. Tel.: +33(0)-320-964-024. Fax: +33(0)-320-964-709. E-mail: benoit.deprez@univ-lille2.fr.

[†] INSERM U761; Université Lille 2; Institut Pasteur de Lille.

[‡] USM504/EA3335 Muséum National d'Histoire Naturelle.

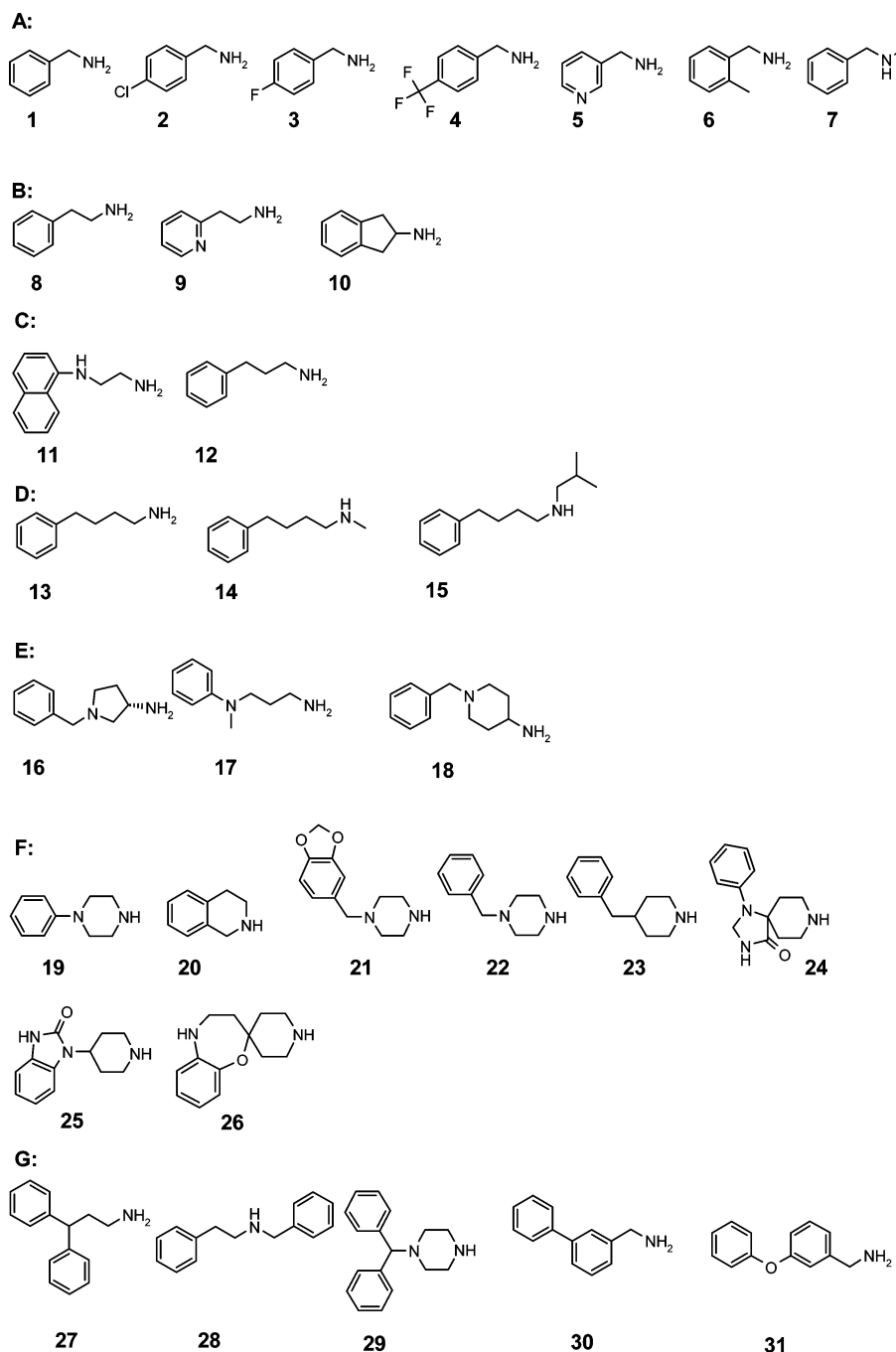


Figure 2. Amine series used for library synthesis.

Table 1. Percentage of Library Members in the Corresponding Range of Inhibition of PfA-M1, Sorted by R₁ Group

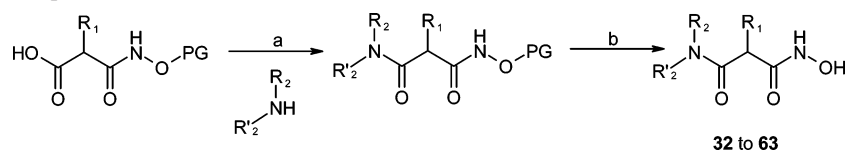
R ₁	range of % inhibition at 10 μM		
	<50%	[50–80%]	>80%
H	96	2	2
<i>i</i> -butyl	60	24	16
benzyl	49	25	26
<i>m</i> -phenoxy-benzyl	43	24	33
NH ₂	94	6	0

products of globin degradation in the food vacuole. Hemoglobin digestion is an important process for the generation and regulation of free amino acids that are used for protein anabolism and for maintaining osmotic stability within the infected erythrocyte. Because there is no detectable aminopeptidase activity in the food vacuole, it is probable that globin degradation

Table 2. Percentage of Library Members in the Corresponding Range of Inhibition of PfA-M1, Sorted by Series of Amine Building Blocks

series of amines	range of % inhibition at 10 μM		
	<50%	[50–80%]	>80%
A	54	13	33
B	77	13	10
C	44	28	28
D	60	20	20
E	73	27	0
F	81	11	8
G	65	24	11

does not go to completion in the food vacuole and that small oligo and dipeptides need to be hydrolyzed by extracellular aminopeptidases, such as PfA-M1.¹⁶ (2) At the schizont stage, an apparent vesicular readdressing leads to the formation of

Scheme 1. Synthesis of Compounds **32** to **63**^a

^a Reagents and conditions: (a) acid 0.5 M/DMF (1 equiv), DIEA (1.1 equiv), CDI (1.1 equiv) 0.25 M/THF, 2 h, rt, then amine 0.1 M/DMF (1 equiv), DIEA (2 equiv), rt, 2 h; or acid 0.5 M/DMF (1 equiv), DIEA (1.2 equiv), and PyBrop 0.2M/DCM (1.2 equiv) 30 s, rt, then amine 0.1 M/DMF (1 equiv), DIEA (2 equiv), rt, overnight; or acid 0.1 M/DMF (1 equiv), DIEA (2.4 equiv), EDCI (1.1 equiv), HOBt (1.1 equiv), rt, 5 min then amine 0.1 M/DMF (1 equiv), DIEA (2 equiv), rt, 5 h; (b) BTFA 0.75M/TFA 0.4% H₂O (25 equiv), 0 °C to rt, 4–6 h or TFA 2%/DCM (0.03 M) and triisopropylsilane, rt, 5 min.

Table 3. Inhibition of PfA-M1 by *iso*-Butyl Compounds **32**–**41**

Cpd	R-	IC ₅₀ ^a (nM)
32		495
33		885
34		790
35		1149
36		406
37		109
38		3896
39		904
40		91
41		45

^a Mean of two experiments. SD was <10% in most cases.

strong fluorescence spots in the merozoites, suggesting a role in the reinvasion of erythrocytes, in agreement with the observation of Kitjaroenthan et al.³⁶ Among metallo-aminopeptidases identified in *P. falciparum* and expressed during the erythrocytic stage, the zinc aminopeptidase PfA-M1 is the first enzyme characterized at the protein level.^{31,35} It is, therefore, an attractive candidate to initiate a program of screening and lead optimization.³⁷

Our group has already described three nonpeptidic, nonselective inhibitors of PfA-M1, with a mixed mode of action.³⁸ Our goal is to identify a selective and potent series of inhibitors of PfA-M1 by screening a library targeting the metalloprotease family.³⁹ We report here the identification of several potent and selective PfA-M1 inhibitors and describe structure–activity relationships in these series. Further optimization produced a

Table 4. Inhibition of PfA-M1 by *m*-Phenoxy-benzyl Compounds **42**–**48**

Cpd	R-	IC ₅₀ ^a (nM)
42		164
43		527
44		225
45		248
46		966
47		130
48		231

^a Mean of two experiments. SD was <10% in most cases.

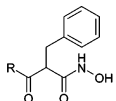
nanomolar, selective inhibitor of PfA-M1, with a good physicochemical and in vitro stability profile that displays a promising antimalarial activity in vitro.

Library

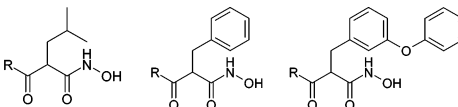
We previously reported the design and synthesis of a diverse library of zinc chelating hydroxamates targeting metalloproteases (Markush formula in Figure 1).³⁹ Amine series (Figure 2) were selected to generate diverse pharmacophoric patterns and geometries. We selected various chain lengths between an aromatic ring and the amino function. Cyclic amines were also incorporated into the library, as well as bulkier amines displaying two phenyl rings. The malonic building blocks (R₁ in Figure 1) were synthesized through various procedures to display a variety of R₁ substituents on the malonic carbon: hydrogen, a polar amino group, and various hydrophobic groups (an isobutyl group and two different aromatic groups) to target diverse metalloproteases. In total, 155 compounds were prepared and screened.

Screening

PfA-M1 was extracted from FcB1 strain as previously described.³⁵ The library of compounds was screened at 10 μM

Table 5. Inhibition of PfA-M1 by Benzyl Compounds 49–63


Cpd	R-	IC ₅₀ ^a (nM)	Cpd	R-	IC ₅₀ ^a (nM)
49		125	57		27
50		1011	58		170
51		125	59		41
52		46	60		107
53		1931	61		2515
54		206	62		1168
55		1760	63		5363
56		253			

^a Mean of two experiments. SD was <10% in most cases.**Table 6.** Influence of the Malonic Substituent on the Inhibition of PfA-M1


R-	Cpd	IC ₅₀ ^a (nM)	Cpd	IC ₅₀ ^a (nM)	Cpd	IC ₅₀ ^a (nM)
	32	495	49	125	42	164
	38	3896	57	27	-	ND
	39	904	58	170	47	130
	34	790	51	125	43	527
	35	1149	52	46	44	225
	36	406	54	206	45	248

^a Mean of two experiments. SD was <10% in most cases. ND: not determined.

against the native enzyme. The enzyme activity was monitored at 405 nm by the release of the chromogenic *p*-nitro-aniline, resulting from the cleavage of the Leu-*p*-nitro-anilide substrate. A *Z'* factor of 0.82 was obtained using these conditions, thus screening was performed in single point determination.⁴⁰ Tables of inhibition percentages are given in the Supporting Information. As expected from an array of hydroxamates, our library yielded a significant numbers of hits on PfA-M1.

Table 7. Inhibition of PfA-M1 and Specificity Toward Mammalian APN of Compounds 40–42, 47, 52, 57, and 59

Cpd	Structure	PfA-M1 inhibition IC ₅₀ ^a (nM)	Mammalian APN inhibition IC ₅₀ ^a (nM)
40		91	8580
41		45	443
42		164	>10,000
47		130	2527
52		46	>10,000
57		27	3616
59		41	1312

^a Mean of two experiments. SD was <10% in most cases.

Statistical Results

Table 1 displays the screening results sorted according to the substituent of the malonic carbon (R₁ in Figure 1). Compounds bearing a benzyl or a *m*-phenoxy-benzyl moiety gave the highest number of hits above 80% of inhibition. The low hit rates obtained for H or NH₂ substituents evidence the need for an isobutyl or better, an aromatic substituent on the malonic chain, to inhibit PfA-M1. Among the aromatic substituents, the *m*-phenoxyphenyl group gives the best activity. Binding of the hydroxamate to the Zn²⁺ ion is expected to be the primary anchoring point of the potential inhibitor. Thus, the enzyme should discriminate more dramatically among substituents close to the hydroxamate than among those remotely bound by a flexible chain. Table 2 displays the screening results sorted according to the amine building-blocks series (R₂ and R'₂ in Figure 1). Several amine series gave lower hit rates than the others: cyclic and constrained amines (series F) and amines with two aromatic groups (series G). Results for other series suggest that the distance between the nitrogen atom and the aromatic ring is critical for inhibition of PfA-M1. Benzylamines (series A), phenylpropylamines (series C), and phenylbutylamines (series D) give higher numbers of hits above 80% of inhibition than phenethylamines (series B). The lowest hit-rates are obtained for amines bearing a tertiary nitrogen atom on the lateral chain (series E). The same library was also screened against mammalian APN^a (neutral aminopeptidase microsomal).

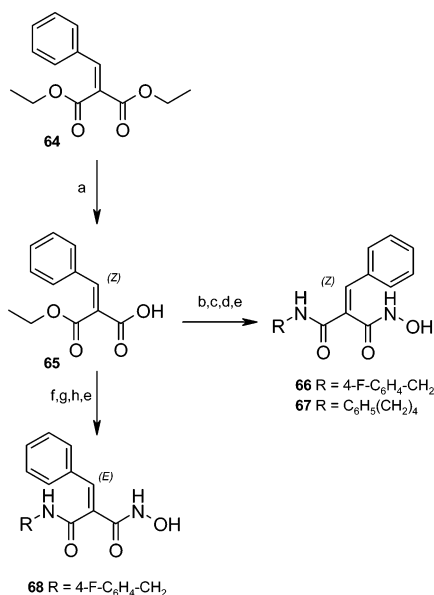
^a Abbreviations: AcOEt, ethylacetate; AcOH, acetic acid; APN, neutral aminopeptidase; BTFA, boron tris(trifluoroacetate); CDI, *N,N'*carbonyldiimidazole; CH₃CN, acetonitrile; DCM, dichloromethane; DIEA, diisopropylethylamine; DMF, dimethylformamide; DMSO, dimethylsulfoxide; EDCl, *N*-ethyl-3-(3-dimethylaminopropyl)carbodiimide; EtOH, ethanol; HOBT, *N*-hydroxybenzotriazole; Leu-*p*NA, leucine-*para*-nitroanilide; MeOH, methanol; PyBrop, bromo-trispyrrolidinophosphonium hexafluorophosphate; TEA, triethylamine; TFA, trifluoroacetic acid; THF, tetrahydrofuran.

Table 8. Activities and Preliminary ADME Parameters of Compounds **52**, **57**, **66**–**68**, **71**, and **72**

cpd	PfA-M1 inhibition IC ₅₀ (nM)	mammalian APN inhibition IC ₅₀ (nM)	solubility ^a (μM)	LogD ^a (pH = 7.4)	plasma stability ^b (hrs)
57	27	3616	>200	1.2	0.75
66	6	1372	198	1.1	22
68	330	> 10 000	ND ^c	ND ^c	ND ^c
71	> 10 000	> 10 000	ND ^c	ND ^c	>48

cpd	PfA-M1 inhibition IC ₅₀ (nM)	mammalian APN inhibition IC ₅₀ (nM)	solubility ^a (μM)	LogD ^a (pH = 7.4)	plasma stability ^b (hrs)
52	46	> 10 000	ND ^c	ND ^c	ND ^c
67	13	3238	ND ^c	ND ^c	ND ^c
72	> 10 000	> 10 000	ND ^c	ND ^c	ND ^c

^a Solubility and LogD are measured from a DMSO stock solution. ^b Half-life rat plasma stability at 37 °C using LC-MS-MS (MRM detection mode). ^c ND = not determined.

Scheme 2. Synthesis of Compounds **66**–**68**^a

^a Reagents and conditions: (a) LiOH (1 equiv), THF, H₂O, 4 h, rt; (b) (i) 1.2 equiv oxalylchloride, DCM, cat. DMF, 45 min, 0 °C; (ii) 3 equiv DIEA, 0.85 equiv *O*-tritylhydroxylamine, DCM, 0 °C then rt, 3 h; (c) 4 equiv LiOH, THF, H₂O, overnight, rt, isomerization; (d) (i) 1.1 equiv ethylchloroformate, 1.1 equiv TEA, DCM, 30 min, 0 °C; (ii) 1.1 equiv 4-fluorobenzylamine or phenylbutylamine, 1 h, rt; (e) TFA 2%/DCM, triisopropylsilane, 5 min, rt; (f) (i) 1.1 equiv ethylchloroformate, 1.1 equiv TEA, DCM, 30 min, 0 °C; (ii) 1 equiv 4-fluorobenzylamine, DCM, 1 h, rt, isomerization; (g) 4 equiv LiOH, THF, H₂O, overnight, rt; (h) (i) 1.1 equiv ethylchloroformate, 1.1 equiv TEA, DCM, 30 min, 0 °C; (ii) 0.85 equiv *O*-tritylhydroxylamine, 1 h, rt.

In this case, results were less clear-cut, suggesting that selectivity against APN, which belongs to the host and should be left intact, can be tractable.³⁹

Structure–Activity Relationships

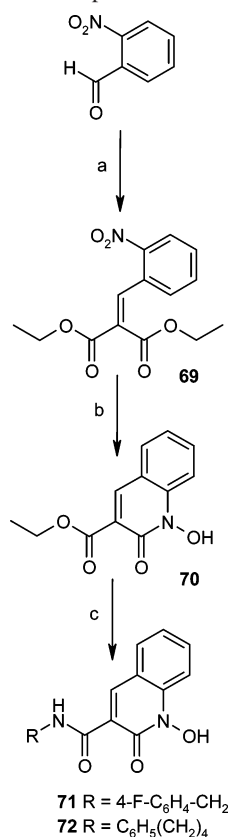
Library members displaying a percentage of inhibition above 80% were selected for resynthesis and further biological characterization (dose response curve and IC₅₀ determination). Some structurally close but less active library members were prepared as well to support structure–activity relationships. Only results with these purified and characterized compounds will be used in the following discussion. Two protocols were used for the synthesis of the compounds depending on the protecting group of the malonic precursor (Scheme 1).³⁹

A rapid analysis shows that SARs depend primarily on the nature of the substituent of the malonic carbon. IC₅₀ values given in Tables 3–5 summarize results for compounds incorporating, respectively, an isobutyl, a benzyl, and a *m*-phenoxy-benzyl substituent on the malonic carbon. Table 6 allows a comparison between the malonic substituents.

Compounds Bearing an Isobutyl on the Malonic Carbon (Table 3). The length and conformation of the carbon chain between the nitrogen of the amine and the aromatic ring appears to be critical for bioactivity (compounds **32**–**35**, and **38**–**41**). Globally, the best activities are obtained for arylmethyl chains.

Compounds **36** and **37** are cyclic analogues of **35**. Both are more active than **35**. Compound **37** is 4 times more active than **36**. This may be due to the hydrogen remaining on the amide function or to its more constrained structure.

In the *N*-benzyl series, substitution at the para position on the benzyl ring of **32** seems to be critical. A fluorine or chlorine atom, in compounds **38** and **39**, leads to a decrease of activity. This decrease is more pronounced for fluorine, suggesting that steric hindrance is not the only factor affecting the binding of the aromatic ring. Compound **37** is an analogue of reduced flexibility of both **32** and **35**. Interestingly, it represents the intersection between the conformational spaces of **32** and **35**, and it is more active than these two compounds (IC₅₀ = 109 nM).

Scheme 3. Synthesis of Compounds **71** and **72**^a

^a Reagents and conditions: (a) 1.2 equiv diethylmalonic ester, 0.4 equiv acetic acid, 0.12 equiv piperidine, benzene, 72 h, reflux; (b) PtO_2 , H_2 , AcOH, 24 h, rt; (c) 4-fluorobenzylamine or 4-phenylbutylamine, 4 h, 60 °C.

In contrast with the results described above, larger groups are tolerated in the meta position (compounds **40** and **41**). In this series, compound **41** bearing a 3-phenoxybenzylamine group has the best activity ($\text{IC}_{50} = 45$ nM).

Compounds Bearing a 3-Phenoxy-benzyl on the Malonic Carbon (Table 4). In the *N*-(phenylalkyl) series, chain length with one or four methylene groups is preferred. Compound **43** is 2.5 times less active than benzylamine and phenylbutylamine analogues (**42** and **44**, respectively). Interestingly, cyclic compound **45** displays an activity similar to its noncyclic analogue **44**, whereas cyclization of benzylamine (**42**) into 1,2,3,4-tetrahydroisoquinoline (**46**) strongly affects activity, compound **46** being 6 times less active than **42**. This suggests that both flexibility and distance between the nitrogen atom and the aryl moiety are important criteria for the activity in this series. Substitution of the benzyl ring by a chlorine atom or a trifluoromethyl group in the para-position (compounds **47** and **48**) appears to impact only slightly on the activity, in contrast with the previous series. In this series, compounds **42** and **47** display the best activities (164 and 130 nM, respectively).

Compounds Bearing a Benzyl on the Malonic Carbon (Table 5). In the *N*-(phenylalkyl) series (compounds **49**–**52**), the longest chain (compound **52**) gives the best activity. Shortening the chain to two methylene groups (compound **50**) leads to a marked decrease of activity. This observation is confirmed with compound **53**, a cyclic analogue of **50**. This suggests that distance between the nitrogen atom and the aryl moiety is an important criterion for the activity.

Constrained compound **54** is four times less active than its flexible analogue (**52**), derived of phenylbutylamine. Interestingly, in this series the replacement of piperidine of compound

Table 9. Antimalarial Activities of **57** and **66**

cmpd	PfA-M1 inhibition IC_{50} (nM)	selectivity ratio (IC_{50} APN/ IC_{50} PfA-M1)	FcB1 ^a IC_{50} ^b (μM)	F32 ^c IC_{50} ^b (μM)
57	27	134	59	57
66	6	229	24	13

^a FcB1: chloroquine-resistant strain. ^b Inhibition of parasite growth; mean of at least three experiments. ^c F32: chloroquine-sensitive strain.

54 by piperazine (compound **55**) leads to a 10-fold decrease in activity. Introduction of larger groups (compounds **61**–**63**) leads to a sharp decrease of activity.

Introducing a constraint via cyclization of benzylamine (**49**) into 1,2,3,4-tetrahydroisoquinoline (**56**) leads to a small loss of activity. Interestingly, substitution on the benzyl ring of **49** is allowed: *p*-chlorobenzylamine (compound **58**) and 1-naphthalenemethylamine (compound **60**) have the same activity as benzylamine (compound **49**), whereas introduction of a fluorine atom in the para-position (compound **57**) or a methyl group in the ortho-position (compound **59**) strongly increases activity. The impact of chlorine on activity is in sharp contrast with the results obtained for compounds in other series. Compound **57** with a *p*-fluoro-benzylamine group is the most active compound ($\text{IC}_{50} = 27$ nM) in our array.

Table 6 summarizes the influence of the malonic substituent on the activity of PfA-M1. Isobutyl derivatives display a lower activity than their aromatic counterparts. This suggests that an aromatic substituent on the malonic chain is necessary to improve the activity of the inhibitors. In all cases, compounds bearing a benzyl group on the malonic carbon display better or same activities than compounds bearing *m*-phenoxybenzyl group. The best hit, **57**, derives from benzylmalonic acid and displays an IC_{50} of 27 nM on the target. It is 150 times more active than its analogue **38** bearing an isobutyl side chain.

Specificity. We also evaluated the specificity (IC_{50}) of some compounds against the mammalian APN to identify potential interactions with host biology (Table 7). As expected from previous results on screening on APN, isobutyl derivatives tend to be less specific for PfA-M1 than benzyl derivatives.³⁹ The most important result is that compounds **52** and **57**, which are the most active inhibitors of PfA-M1, are also highly selective.

Optimization of **52 and **57** and Antimalarial Activity.** To increase the activity on the target and to remove the chiral carbon (malonic), we synthesized unsaturated analogues of **52** and **57**: compounds **66**–**68** and **71** and **72** (Schemes 2 and 3, respectively). Carboxylic acid **65** was obtained from the corresponding ethyl ester using LiOH in a mixture of THF and H_2O (Scheme 2). The configuration of this acid was determined by a nondecoupled ^{13}C NMR experiment. Further reaction of **65** with *O*-trityl-hydroxylamine, hydrolysis of the residual ester function, and reaction with the desired amines gave compounds **66** and **67**. ROESY experiments allowed us to attribute a *Z* configuration to **66** and **67**. *E*-Isomer **68** was obtained from the same intermediate **65** by reversing the sequence of introduction of the amine and the protected hydroxylamine (Scheme 2). Cyclic compounds **71** and **72** were obtained in three steps (Scheme 3). First, *o*-nitro-benzaldehyde and diethylmalonate react in a classical Knoevenagel reaction. Then **70** is obtained via a one-pot reduction and cyclization.⁴¹ Finally, aminolysis of the remaining ester function, with the corresponding amines, yielded **71** and **72** (Scheme 3). The determination of the activities of these compounds allowed expanding our structure–activity relationships.

While cyclization of **52** and **57** (respectively, compounds **72** and **71**) is detrimental for the inhibition of the target (Table 8), introduction of an insaturation with a *Z* configuration at the malonic carbon increases the activity on PfA-M1 (compounds **66** and **67**; Table 8). Selectivity is either maintained (**67** vs **52**) or enhanced (**66** vs **57**). In the 4-fluorobenzyl series, *E*-isomer **68** is 12 times less active than the saturated **57** and 55 times less active than *Z*-isomer **66**. Nevertheless, **66** and **68** are both selective of PfA-M1 versus APN. Compound **66** displays the best activity on the target ($IC_{50} = 6$ nM).

Various parameters were calculated for compounds **52**, **57**, **66–68**, **71**, and **72** to evaluate drug-likeness: molecular weight, 312–340; HBD, 2 or 3; HBA, 3; PSA, 70–86; and bioavailability score ABS, 0.55.⁴² Solubility and LogD (pH 7.4) were measured for **57** and **66** and found acceptable (Table 8). Plasma stability at 37 °C was measured for compounds in the 4-fluorobenzyl series **57**, **66**, and **71** using LC-MS-MS. Electronic and steric environment of the hydroxamic acid function, here insaturation and cyclization, strongly influences the stability as previously observed.^{43,44} In plasma, compound **57** is hydrolyzed to carboxylic acid, with a half-life of 45 min. Cyclization in 1-hydroxy-2-oxo-1,2-dihydroquinoline prevents hydrolysis to carboxylic acid and stabilizes compound **71** ($t_{1/2} > 48$ h). Interestingly, introduction of the double bond (compound **66**) further increases stability ($t_{1/2} = 22$ h). Generally, these preliminary ADME studies confirmed that this series, and compound **66** in particular, displays reasonable drug-like properties and deserves further biological characterization.

The best inhibitor **57** directly issued from screening and its optimized analogue **66** were tested on *Plasmodium falciparum* FcB1 and F32 strains (Table 9). Both compounds demonstrated an inhibition of parasite growth in the order of magnitude of some previously reported inhibitors of plasmepsins or falcipains.^{19–23} The differences of activity between the inhibition of PfA-M1 and the in vitro antimalarial activity may be due to low cell permeation or trapping of these compounds in red blood cells by carbonic anhydrase, a zinc metallo-enzyme found at a high cellular concentration in red blood cells.⁴⁵ Other analogues are currently being synthesized to optimize cell permeation. Compound **66**, more active on PfA-M1 and more stable than **57**, is also twice as active as its analogue. Both compounds display good (>100 fold) selectivity toward the related mammalian enzyme APN.

Conclusion

We have screened a library of hydroxamates with a malonic scaffold for its inhibition of PfA-M1, a zinc amino-peptidase of the M1 family of *Plasmodium falciparum*. Several inhibitors displaying promising in vitro activity on the enzyme have been identified. Furthermore, most of them showed the desired specificity against APN, the host M1 family prototype. Especially, we have identified compound **57** as a promising hit, displaying activity on *Plasmodium falciparum* FcB1 and F32 strains. Further optimization produced **66**, the best inhibitor of PfA-M1 so far described, which demonstrated antiparasitodal activity.

Experimental Section

Biology. Inhibition of PfA-M1. Native PfA-M1 (FcB1 strain) was purified according to the procedure described by Allary et al.³⁵ and diluted 10 times in Tris–HCl buffer (25 mM; pH 7.4) before use. The assays were set up in 96-well plates. The compounds were tested at the concentration of 10 μ M. An amount equal to 33 μ L of purified PfA-M1 was preincubated 10 min at room temperature with 33 μ L of the inhibitor (30 μ M in Tris–HCl buffer, 0.3%

DMSO). An amount equal to 33 μ L of the substrate Leu-pNA ($K_m = 0.099$ mM), 0.3 mM in Tris–HCl buffer, was then added. The reaction kinetics performed at room temperature was followed on a UV-microplate reader MultiskanRC (Labsystems, Finland) at 405 nm. The control activity was determined by incubating the enzyme in the same conditions without inhibitor. Bestatin was used as the reference inhibitor ($IC_{50} = 284$ nM). The statistical *Z'* factor for the test was 0.82, allowing activities to be determined with a single point with a 95% confidence.⁴⁰ Initial velocities are expressed in μ mol·min⁻¹. Data were normalized to the controls that represent V_{max} . For the determination of IC_{50} values, initial velocities were plotted as a function of inhibitor concentration using XLfit software from IDBS.

Inhibition of APN. Microsomal APN from porcine kidney was purchased from Sigma, Inc., as an ammonium sulfate suspension (3.5 M (NH₄)₂SO₄ solution containing 10 mM MgCl₂), 10–40 units/mg protein. The enzyme suspension was diluted 600-fold in Tris–HCl buffer (25 mM; pH = 7.4) before use. The assays were performed in 96-well plates. The compounds were tested at the concentration of 10 μ M. Purified APN (33 μ L) was preincubated 10 min at room temperature with 33 μ L of the inhibitor (30 μ M in Tris–HCl buffer, 0.3% DMSO). The substrate Leu-pNA (33 μ L; $K_m = 0.099$ mM), 0.3 mM in Tris–HCl buffer, was then added. The reaction kinetics performed at room temperature was followed on a UV-microplate reader MultiskanRC (Labsystems, Finland) at 405 nm. The control activity was determined by incubating the enzyme in the same conditions without inhibitor. Bestatin was used as the reference inhibitor ($IC_{50} = 2.7$ μ M). The statistical *Z'* factor for the test was 0.75, allowing activities to be determined with a single point with a 95% confidence.⁴⁰ Initial velocities are expressed in μ mol·min⁻¹. Data were normalized to the controls that represent V_{max} . For the determination of IC_{50} values, initial velocities were plotted as a function of inhibitor concentration, using XLfit software from IDBS.

Parasite Growth Inhibition. *P. falciparum* strains were maintained continuously in culture on human erythrocytes, as described by Trager and Jensen.⁴⁶ In vitro antiparasitodal activity was determined using a modification of the semiautomated microdilution technique of Desjardins et al.⁴⁷ *P. falciparum* chloroquine (CQ)-resistant FcB1 (Colombia) strain (CQ: $IC_{50} = 115 \pm 5$ nM) or chloroquine (CQ)-sensitive F32 (Tanzania) strain (CQ: $IC_{50} = 21 \pm 5$ nM) was used. Stock solutions of test compounds were prepared in sterile distilled water and DMSO, respectively. Drug solutions were serially diluted with culture medium and introduced to asynchronous parasite cultures (0.5% parasitemia and 1% final hematocrite) on 96-well plates for 24 h at 37 °C prior to the addition of 0.5 mCi of [³H]hypoxanthine (1–5 Ci/mmol; Amersham, France) per well. The growth inhibition of each drug concentration was determined by comparison of the radioactivity incorporated into the treated culture with that in the control culture (without drug) maintained on the same plate. The IC_{50} value, as obtained from the drug concentration–response curve, was expressed as the mean of three independent experiments, SD were <10% in most cases. The DMSO concentration never exceeded 0.1% and did not inhibit the parasite growth.

Solubility. Log D. Plasma Stability. These experiments used a LC-MS-MS triple-quadrupole system (Varian 1200ws) under MRM detection using the following mass parameters: mode of ionization, electrospray; declustering potential, 50 V; collision-activated dissociation, 1.5 mTorr; collision energy, 20 eV. Transitions observed were, respectively: **57** (317 > 109); **66** (315 > 109); **71** (313 > 109).

Solubility. The 10 mM solution (40 μ L) in DMSO of the sample was added to 1.960 mL of MeOH or PBS at pH = 7.4. The samples were gently shaken for 24 h at room temperature, then centrifuged for 5 min, and filtered over 0.45 μ m filters. An amount equal to 20 μ L of each solution was added to 180 μ L of MeOH and analyzed by LC-MS-MS. The solubility was determined by the ratio of mass signal areas PBS/MeOH.

Log D. A 40 μ L aliquot of the 10 mM solution in DMSO of the sample was added to 1.960 mL of a 1/1 octanol/PBS at pH = 7.4

solution. The mixture was gently shaken for 2 h at room temperature, then the two phases were separated. A 20 μL aliquot of each solution was added to 180 μL of MeOH and analyzed by LC-MS-MS. Log D was determined as the logarithm of the ratio of concentrations of product in octanol and PBS, determined by mass signals.

Plasma Stability. A 40 μL aliquot of the 5 mM solution in DMSO of the sample was added to 1.960 mL of rat plasma (male Zucker rat FA/FA plasma from Charles River Laboratories) to obtain a 100 μM final solution. The mixture was gently stirred 96 h at 37 °C. Aliquots of 200 μL were taken at various times (from 0 to 96 h) and diluted with 200 μL of phosphoric acid (0.14 M). A 10 μL aliquot of the 2 mM solution in methanol of the internal standard was added. Compounds were extracted three times with 2 mL of AcOEt. The organic layer was evaporated, diluted with 200 μL of methanol, and quantified by LC-MS-MS using a calibration curve.

Chemistry. General Information. NMR spectra were recorded on a Bruker DRX-300 spectrometer. Chemical shifts are in parts per million (ppm). The assignments were made using one-dimensional (1D) ^1H and ^{13}C spectra and two-dimensional (2D) HSQC and COSY spectra. Mass spectra were recorded on a MALDI-TOF Voyager-DE-STR spectrometer or with a LC-MS-MS triple-quadrupole system (Varian 1200ws). HPLC analysis was performed using a C18 TSK-GEL Super ODS 2 μm particle size column, dimensions 50 \times 4.6 mm. A gradient starting from 100% $\text{H}_2\text{O}/0.05\%$ TFA and reaching 20% $\text{H}_2\text{O}/80\%$ $\text{CH}_3\text{CN}/0.05\%$ TFA within 10 min at a flow rate of 1 mL/min was used. LCMS gradient starting from 100% $\text{H}_2\text{O}/0.1\%$ formic acid and reaching 20% $\text{H}_2\text{O}/80\%$ $\text{CH}_3\text{CN}/0.08\%$ formic acid within 10 min at a flow rate of 1 mL/min was used. Melting points were determined on a Büchi B-540 apparatus and are uncorrected. All commercial reagents and solvents were used without further purification. Organic layers obtained after extraction of aqueous solutions were dried over MgSO_4 and filtered before evaporation in vacuo. Purification yields were not optimized. Bond-Elut SAX-columns were purchased from Varian, Inc. All the 5 μmol scale reactions were performed in 96-well (round-bottomed) polypropylene plates (1200 μL).

Synthesis from *N*-tert-Butoxy-malonamic Acids Using PyBrop as Coupling Agent (Method A): Synthesis of *N*-tert-butoxy-malonamic acid precursors is described in reference 36. Carboxylic acid (0.5 M/DMF; 1 equiv), DIEA (1.2 equiv), and PyBrop (0.2 M/DCM; 1.2 equiv) were stirred 30 s at room temperature. Then the appropriate amine (0.1 M/DMF; 1 equiv) and DIEA (2 equiv) were added, the mixture was stirred overnight at room temperature, and then solvents were removed under reduced pressure. The residue was dissolved in DCM, and the organic phase was washed with aqueous HCl 1 N (3 times), aqueous NaHCO_3 5% (3 times), and water (once). The organic layer was dried over MgSO_4 and evaporated under reduced pressure. The residue was purified by thick layer chromatography on silica gel (DCM/MeOH 95/5).

Synthesis from *N*-Trityl-oxymalonamic Acids Using CDI as Coupling Agent (Method B): Synthesis of *N*-trityloxy-malonamic acid precursors is described in reference 36. Carboxylic acid (0.5 M/DMF; 1 equiv), DIEA (1.1 equiv), and *N,N'*-carbonyldiimidazole (0.25 M/THF; 1.1 equiv) were stirred 2 h at room temperature. Then the appropriate amine (0.1 M/DMF; 1 equiv) and DIEA (2 equiv) were added, the mixture was stirred 2 h at room temperature, and then solvents were removed under reduced pressure. The residue was dissolved in the minimum AcOEt, and the organic phase was washed with aqueous KHSO_4 (pH = 3) and water (3 times). The organic layer was dried over MgSO_4 and evaporated under reduced pressure. The residue was purified on Bond-Elut SAX column using DCM to remove residual carboxylic acid. The powder obtained was triturated in ether–pentane.

Synthesis from *N*-Trityl-oxymalonamic Acids Using HOBt/EDCI as Coupling Agents (Method C): Synthesis of *N*-trityloxy-malonamic acid precursors is described in reference 36. Carboxylic acid (0.1 M/DMF; 1 equiv), DIEA (2.4 equiv), EDCI (1.1 equiv), and HOBt (1.1 equiv) were stirred 5 min at room temperature. Then the appropriate amine (0.1 M/DMF; 1 equiv) and DIEA (2 equiv)

were added. The mixture was stirred 5 h at room temperature and then solvents were removed under reduced pressure. The residue was dissolved in AcOEt and the organic phase was washed with aqueous NaHCO_3 5% (6 times) and NaCl (once). The organic layer was dried over MgSO_4 and evaporated under reduced pressure. The residue was precipitated in petroleum ether.

tert-Butyl Deprotection: *tert*-Butylated intermediate was dissolved in a suspension of BTFA (0.75 M/TFA; 25 equiv) with 0.4% H_2O . The reaction mixture was stirred 4 h to 5 h 30 min at room temperature. Solvents were removed under reduced pressure and the residue was dissolved in water. The aqueous phase was basified with NaOH 1 M to pH = 7 and extracted three times with AcOEt. The organic layers were dried over MgSO_4 , filtered, and evaporated. The residue was precipitated in ether–pentane. Yields given are those of the deprotection step.

Trityl Deprotection: Tritylated intermediate was dissolved in TFA 2%/DCM and triisopropylsilane was added drop by drop until the yellow color disappeared. The reaction mixture was stirred 5 min at room temperature, solvents were removed under reduced pressure, and the residue was washed with ether–pentane. Yields given are those of the deprotection step.

***N*-Benzyl-*N'*-hydroxy-2-isobutyl-malonamide (32; Method B):** White powder; yield 75%; purity 100%; ^1H NMR (DMSO- d_6) δ 0.85 (d, J = 6.0 Hz, 6H), 1.39–1.52 (m, 1H), 1.53–1.70 (m, 2H), 3.04 (t, J = 7.5 Hz, 1H), 4.26 (d, J = 5.7 Hz, 2H), 7.21–7.34 (m, 5H), 8.15 (t, J = 5.7 Hz, NHCO), 8.97 (s, 1H, OH), 10.53 (s, 1H, CONHO); ^{13}C NMR (DMSO- d_6) δ 22.6, 23.0, 26.0, 38.9, 42.7, 49.4, 127.2, 127.5, 128.7, 139.8, 167.2, 169.5; $t_{\text{R(LCMS)}}$ 3.90 min; MS (MH) $^+$ m/z 265 and (MNa) $^+$ m/z 287.

***N*-Hydroxy-2-isobutyl-*N'*-phenethyl-malonamide (33; Method B):** White powder; yield 74%; purity 100%; ^1H NMR (DMSO- d_6) δ 0.82 (d, J = 6.6 Hz, 6H), 1.30–1.43 (m, 1H), 1.45–1.58 (m, 2H), 2.69 (t, J = 7.2 Hz, 2H), 2.94 (t, J = 7.5 Hz, 1H), 3.27 (q, J = 6.9 Hz, 2H), 7.18–7.31 (m, 5H), 7.68 (t, J = 5.7 Hz, NHCO), 8.94 (s, 1H, OH), 10.47 (s, 1H, CONHO); $t_{\text{R(LCMS)}}$ 4.11 min; ^{13}C NMR (DMSO- d_6) δ 22.6, 22.9, 25.9, 35.5, 39.2, 41.0, 49.4, 126.5, 128.7, 129.1, 139.8, 167.3, 169.3; MS (MH) $^+$ m/z 279 and (MNa) $^+$ m/z 301.

***N*-Hydroxy-2-isobutyl-*N'*-(3-phenyl-propyl)-malonamide (34; Method B):** White powder; yield 75%; purity 100%; ^1H NMR (DMSO- d_6) δ 0.85 (d, J = 6.0 Hz, 6H), 1.38–1.51 (m, 1H), 1.55–1.73 (m, 4H), 2.48–2.52 (m, 2H), 2.98 (t, J = 7.5 Hz, 1H), 3.00–3.07 (m, 2H), 7.18–7.31 (m, 5H), 7.69 (br s, NHCO), 8.93 (s, 1H, OH), 10.47 (s, 1H, CONHO); ^{13}C NMR (DMSO- d_6) δ 22.6, 22.9, 26.1, 31.3, 32.9, 38.7, 38.9, 49.5, 126.2, 128.7, 128.8, 142.1, 167.3, 169.4; $t_{\text{R(LCMS)}}$ 4.63 min; MS (MH) $^+$ m/z 293.

***N*-Hydroxy-2-isobutyl-*N'*-(4-phenyl-butyl)-malonamide (35; Method A):** The compound was deprotected using TFA 80%/DCM, room temperature, 72 h. It was purified by reverse-phase preparative HPLC and lyophilized; white powder; yield 7%; purity 100%; ^1H NMR (DMSO- d_6) δ 0.75 (dd, J = 1.2 Hz, J = 6.5 Hz, 6H), 1.28–1.35 (m, 3H), 1.40–1.50 (m, 4H), 2.48 (t, J = 7.3 Hz, 2H), 2.87 (t, J = 7.5 Hz, 1H), 2.95–3.00 (m, 2H), 7.07–7.12 (m, 3H), 7.16–7.20 (m, 2H), 7.54 (t, J = 5.7 Hz, NHCO), 8.82 (br s, OH), 9.30 (br s, CONHO); $t_{\text{R(LCMS)}}$ 5.10 min; MS (MH) $^+$ m/z 307.

2-(4-Benzyl-piperidine-1-carbonyl)-4-methyl-pentanoic Acid Hydroxyamide (36; Method C): White powder; yield 30%; purity 100%; ^1H NMR (CD_2Cl_2) δ 0.91–0.98 (m, 6H), 1.11–1.22 (m, 2H), 1.55–1.59 (m, 1H), 1.61–1.82 (m, 5H), 2.52–2.59 (m, 3H), 3.03 (t, J = 12.9 Hz, 1H), 3.73 (t, J = 7.0 Hz, 1H), 3.98 (d, J = 13.2 Hz, 1H), 4.58 (d, J = 12.9 Hz, 1H), 7.16–7.24 (m, 3H), 7.29–7.34 (m, 2H); $t_{\text{R(LCMS)}}$ 5.30 min; MS (MH) $^+$ m/z 333.

***N*-Hydroxy-2-isobutyl-*N'*-(1,2,3,4-tetrahydro-naphthalen-1-yl)-malonamide (37; Method B):** White powder; yield 24%; purity 100%; mixture of the cis and trans form of the amide function; ^1H NMR (DMSO- d_6) δ 0.86 (d, J = 6.3 Hz, 6H), 1.42–1.86 (m, 7H), 2.64–2.82 (m, 2H), 3.01–3.08 (m, 1H), 4.91–4.94 (m, 1H), 7.09–7.17 (m, 4H), 7.95 (d, J = 8.4 Hz, 0.6H, NHCO), 7.99 (d, J = 8.4 Hz, 0.4H, NHCO), 8.96 (s, 1H, OH), 10.42 (s, 1H, CONHO); $t_{\text{R(LCMS)}}$ 4.71 min; MS (MH) $^+$ m/z 305.

***N*-(4-Fluoro-benzyl)-*N'*-hydroxy-2-isobutyl-malonamide (38; Method A):** Beige powder; yield 15%; purity 95%; ¹H NMR (DMSO-*d*₆) δ 0.85 (d, *J* = 5.4 Hz, 6H), 1.39–1.67 (m, 3H), 3.03 (t, *J* = 7.5 Hz, 0.7H), 3.19 (t, *J* = 6.9 Hz, 0.3H), 4.24 (d, *J* = 5.7 Hz, 2H), 7.12–7.17 (m, 2H), 7.25–7.29 (m, 2H), 8.17 (t, *J* = 5.7 Hz, 0.7H, NHCO), 8.40 (s, 0.3H, NHCO), 8.96 (s, 1H, OH), 10.54 (s, 1H, CONHO); *t*_{R(LCMS)} 4.13 min; MS (MH)⁺ *m/z* 283.

***N*-(4-Chloro-benzyl)-*N'*-hydroxy-2-isobutyl-malonamide (39; Method A):** White powder; yield 30%; purity 95%; ¹H NMR (DMSO-*d*₆) δ 0.85 (d, *J* = 6.3 Hz, 6H), 1.42–1.64 (m, 3H), 3.03 (t, *J* = 7.5 Hz, 0.5H), 3.20 (t, *J* = 6.3 Hz, 0.5H), 4.24 (d, *J* = 6 Hz, 2H), 7.23–7.39 (m, 4H), 8.20 (t, *J* = 6.0 Hz, 0.5H, NHCO), 8.43 (m, 0.5H, NHCO), 8.96 (s, 1H, OH), 10.55 (s, 1H, CONHO); *t*_{R(LCMS)} 4.65 min; MS (MH)⁺ *m/z* 299.

***N*-Hydroxy-2-isobutyl-*N'*-naphthalen-1-ylmethyl-malonamide (40; Method A):** Beige powder; yield 59%; purity 95%; ¹H NMR (DMSO-*d*₆) δ 0.85 (d, *J* = 6.3 Hz, 6H), 1.41–1.50 (m, 1H), 1.64 (t, *J* = 6.9 Hz, 2H), 3.08 (t, *J* = 7.5 Hz, 1H), 4.68 (dd, *J* = 5.4, *J* = 15.3 Hz, 1H), 4.79 (dd, *J* = 5.4, *J* = 15.3 Hz, 1H), 7.43–7.57 (m, 4H), 7.86 (d, *J* = 7.5 Hz, 1H), 7.94–7.97 (m, 1H), 8.04–8.07 (m, 1H), 8.19 (t, *J* = 5.4 Hz, 1H, NHCO), 8.97 (s, 1H, OH), 10.52 (s, 1H, CONHO); *t*_{R(HPLC)} 5.03 min; MS (MH)⁺ *m/z* 315.

***N*-Hydroxy-2-isobutyl-*N'*-(3-phenoxy-benzyl)-malonamide (41; Method B):** White powder; yield 52%; purity 100%; ¹H NMR (DMSO-*d*₆) δ 0.82 (d, *J* = 6.3 Hz, 6H), 1.35–1.44 (m, 1H), 1.51–1.63 (m, 2H), 3.02 (t, *J* = 7.5 Hz, 1H), 4.24–4.27 (m, 2H), 6.85–6.90 (m, 2H), 6.98–7.01 (m, 3H), 7.14 (t, *J* = 7.2 Hz, 1H), 7.32 (t, *J* = 7.8 Hz, 1H), 7.39 (t, *J* = 8.1 Hz, 2H), 8.19 (t, *J* = 5.4 Hz, NHCO), 8.95 (s, 1H, OH), 10.52 (s, 1H, CONHO); *t*_{R(LCMS)} 5.32 min; MS (MH)⁺ *m/z* 357.

***N*-Benzyl-*N'*-hydroxy-2-(3-phenoxy-benzyl)-malonamide (42; Method B):** Beige powder; yield 89%; purity 99%; ¹H NMR (DMSO-*d*₆) δ 2.96–3.10 (m, 2H), 3.29–3.32 (m, 1H), 4.17 (dd, *J* = 15.1 Hz, *J* = 5.2 Hz, 1H), 4.29 (dd, *J* = 15.1 Hz, *J* = 6.1 Hz, 1H), 6.81–7.39 (m, 14H), 8.26 (t, *J* = 5.7 Hz, NHCO), 8.95 (s, OH), 10.47 (s, CONHO); *t*_{R(LCMS)} 5.47 min; MS (MH)⁺ *m/z* 391; mp 164–167 °C.

***N*-Hydroxy-2-(3-phenoxy-benzyl)-*N'*-(3-phenyl-propyl)-malonamide (43; Method B):** White powder; yield 68%; purity 99%; ¹H NMR (DMSO-*d*₆) δ 1.60–1.64 (m, 2H), 2.45–2.50 (m, 2H), 2.95–3.05 (m, 4H), 3.22 (t, *J* = 7.0 Hz, 1H), 6.78–6.95 (m, 5H), 6.99–7.37 (m, 9H), 7.73–7.76 (m, NHCO), 8.93 (s, OH), 10.41 (s, CONHO); ¹³C NMR (DMSO-*d*₆) δ 31.2, 32.8, 34.9, 38.8, 52.6, 116.9, 118.8, 119.7, 123.7, 124.6, 126.2, 128.7, 128.8, 130.1, 130.4, 141.8, 142.1, 156.7, 157.1, 166.2, 168.4; *t*_{R(LCMS)} 5.90 min; MS (MH)⁺ *m/z* 419; mp 126–128 °C.

***N*-Hydroxy-2-(3-phenoxy-benzyl)-*N'*-(4-phenyl-butyl)-malonamide (44; Method B):** White powder; yield 88%; purity 99%; ¹H NMR (DMSO-*d*₆) δ 1.31–1.38 (m, 2H), 1.43–1.50 (m, 2H), 2.52–2.55 (m, 2H), 2.96–3.04 (m, 4H), 3.19 (t, *J* = 7.6 Hz, 1H), 6.78–6.97 (m, 5H), 7.10–7.39 (m, 9H), 7.69 (t, *J* = 5.4 Hz, NHCO), 8.92 (s, OH), 10.39 (s, CONHO); ¹³C NMR (DMSO-*d*₆) δ 28.6, 29.0, 34.9, 35.2, 39.2, 52.6, 117.0, 118.8, 119.7, 123.7, 124.6, 126.1, 128.7, 128.8, 130.1, 130.4, 141.7, 142.5, 156.7, 157.2, 166.2, 168.3; *t*_{R(LCMS)} 6.26 min; MS (MH)⁺ *m/z* 433; mp 131–133 °C.

3-(4-Benzyl-piperidin-1-yl)-*N*-hydroxy-3-oxo-2-(3-phenoxy-benzyl)-propionamide (45; Method B): Beige powder; yield 74%; purity 95%; ¹H NMR (DMSO-*d*₆) δ 0.75–1.04 (m, 2H), 1.38–1.50 (m, 2H), 1.68–1.72 (m, 1H), 2.37–2.50 (m, 4H), 2.78–2.94 (m, 2H), 3.67–3.71 (m, 1H), 3.85–3.92 (m, 1H), 4.27–4.31 (m, 1H), 6.78–7.41 (m, 14H), 10.45 (s, 0.6 CONHO), 10.55 (s, 0.4 CONHO); *t*_{R(LCMS)} 6.50 min; MS (MH)⁺ *m/z* 459; mp 73–77 °C.

3-(3,4-Dihydro-1*H*-isoquinolin-2-yl)-*N*-hydroxy-3-oxo-2-(3-phenoxy-benzyl)-propionamide (46; Method B): Yellow oil; yield 85%; purity 95%; mixture of the *cis* and *trans* form of the amide function (0.6/0.4); ¹H NMR (CD₂Cl₂) δ 2.28–2.37 (m, 0.6H), 2.66–2.77 (m, 1.4H), 3.12–3.32 (m, 2.6H), 3.47–3.64 (m, 1H), 3.79–3.86 (m, 0.4H), 3.96–4.15 (m, 2H), 4.47–4.60 (m, 1H), 6.70–7.34 (m, 13H), 10.23 (s, CONHO); *t*_{R(LCMS)} 5.77 min; MS (MH)⁺ *m/z* 417.

***N*-(4-Chloro-benzyl)-*N'*-hydroxy-2-(3-phenoxy-benzyl)-malonamide (47; Method B):** Beige powder; yield 73%; purity 99%; ¹H NMR (DMSO-*d*₆) δ 3.00–3.06 (m, 2H), 3.30–3.35 (m, 1H), 4.13–4.28 (m, 2H), 6.82–7.36 (m, 13H), 8.27–8.30 (m, NHCO), 8.96 (s, OH), 10.45 (s, CONHO); ¹³C NMR (DMSO-*d*₆) δ 34.9, 42.0, 52.6, 117.0, 118.8, 119.7, 123.7, 124.6, 128.6, 129.3, 130.2, 130.4, 131.6, 138.8, 141.6, 156.8, 157.1, 166.0, 168.6; *t*_{R(LCMS)} 5.82 min; MS (MH)⁺ *m/z* 425; mp 169–171 °C.

***N*-Hydroxy-2-(3-phenoxy-benzyl)-*N'*-(4-trifluoromethyl-benzyl)-malonamide (48; Method B):** White powder; yield 78%; purity 99%; ¹H NMR (DMSO-*d*₆) δ 3.02–3.07 (m, 2H), 3.32–3.37 (m, 1H), 4.26 (dd, *J* = 15.0 Hz, *J* = 4.5 Hz, 1H), 4.36 (dd, *J* = 15.6 Hz, *J* = 5.7 Hz, 1H), 6.82–7.00 (m, 5H), 7.12 (t, *J* = 7.3 Hz, 1H), 7.25–7.39 (m, 5H), 7.60 (d, *J* = 7.8 Hz, 2H), 8.37–8.40 (m, NHCO), 8.97 (s, OH), 10.49 (s, CONHO); ¹³C NMR (DMSO-*d*₆) δ 34.9, 42.3, 52.6, 116.9, 118.8, 119.7, 123.7, 124.6, 124.8 (d, *J*_{CF} = 270 Hz), 125.4 (d, *J*_{CF} = 4 Hz), 127.8 (d, *J*_{CF} = 35 Hz), 128.0, 130.2, 130.4, 141.6, 144.7, 156.8, 157.1, 165.9, 168.7; *t*_{R(LCMS)} 6.05 min; MS (MH)⁺ *m/z* 459; mp 189–191 °C.

2*N*-Dibenzyl-*N'*-hydroxy-malonamide (49; Method C): White powder; yield 84%; purity 100%; ¹H NMR (DMSO-*d*₆) δ 3.00–3.08 (m, 2H), 3.30 (t, *J* = 6.75 Hz, 1H), 4.20 (dd, *J* = 5.1 Hz, *J* = 15 Hz, 1H), 4.30 (dd, *J* = 5.4 Hz, *J* = 15 Hz, 1H), 7.10–7.23 (m, 10H), 8.20–8.23 (m, NHCO), 10.44 (s, CONHO); ¹³C NMR (DMSO-*d*₆) δ 35.1, 42.7, 52.7, 126.6, 127.1, 127.5, 128.6, 128.7, 129.3, 139.4, 139.6, 166.2, 168.6; *t*_{R(LCMS)} 4.25 min; MS (MH)⁺ *m/z* 299; mp 167–169 °C.

2-Benzyl-*N*-hydroxy-*N'*-phenethyl-malonamide (50; Method A): Beige powder; yield 17%; purity 100%; ¹H NMR (DMSO-*d*₆) δ 2.63 (t, *J* = 7.1 Hz, 2H), 2.96 (d, *J* = 7.2 Hz, 2H), 3.17–3.22 (m, 3H), 7.12–7.29 (m, 10H), 8.07 (s, NHCO); *t*_{R(LCMS)} 4.31 min; MS (MH)⁺ *m/z* 313; mp 121–125 °C.

2-Benzyl-*N*-hydroxy-*N'*-(3-phenyl-propyl)-malonamide (51; Method C): White powder; yield 53%; purity 98%; ¹H NMR (DMSO-*d*₆) δ 1.58–1.68 (m, 2H), 2.45–2.50 (m, 2H), 2.99–3.05 (m, 4H), 3.22 (t, *J* = 7.5 Hz, 1H), 7.14–7.29 (m, 10H), 7.74 (t, *J* = 5.4 Hz, NHCO), 8.91 (s, OH), 10.41 (s, CONHO); ¹³C NMR (DMSO-*d*₆) δ 31.2, 32.9, 35.1, 38.8, 52.8, 126.2, 126.6, 128.6, 128.7, 128.8, 129.2, 139.5, 142.1, 166.3, 168.5; *t*_{R(LCMS)} 4.82 min; MS (MH)⁺ *m/z* 327; mp 148–150 °C.

2-Benzyl-*N*-hydroxy-*N'*-(4-phenyl-butyl)-malonamide (52; Method B): White powder; yield 18%; purity 99%; ¹H NMR (DMSO-*d*₆) δ 1.29–1.39 (m, 2H), 1.43–1.53 (m, 2H), 2.53 (t, *J* = 7.5 Hz, 2H), 2.98–3.06 (m, 4H), 3.19 (t, *J* = 7.8 Hz, 1H), 7.16–7.25 (m, 10H), 7.69 (t, *J* = 5.4 Hz, 1H, NHCO), 8.91 (s, 1H, OH), 10.4 (br s, 1H, CONHO); ¹³C NMR (DMSO-*d*₆) δ 28.6, 29.1, 35.1, 35.2, 39.2, 52.8, 126.1, 126.6, 128.6, 128.7, 128.8, 129.2, 139.5, 142.5, 166.3, 168.5; *t*_{R(LCMS)} 5.20 min; MS (MH)⁺ *m/z* 341.

2-Benzyl-*N*-hydroxy-*N'*-indan-2-yl-malonamide (53; Method B): White powder; yield 76%; purity 99%; ¹H NMR (DMSO-*d*₆) δ 2.63 (dd, *J* = 5.4 Hz, *J* = 16 Hz, 1H), 2.75 (dd, *J* = 5.4 Hz, *J* = 16 Hz, 1H), 3.00 (d, *J* = 7.2 Hz, 2H), 3.09 (t, *J* = 7.2 Hz, 1H), 3.16 (dd, *J* = 7.8 Hz, *J* = 15.8 Hz, 2H), 4.35–4.46 (m, 1H), 7.12–7.27 (m, 9H), 7.99 (d, *J* = 7.2 Hz, 1H, NHCO), 8.62 (s, 1H, OH), 10.35 (br s, 1H, CONHO); *t*_{R(LCMS)} 4.92 min; MS (MH)⁺ *m/z* 325.

2-Benzyl-3-(4-benzyl-piperidin-1-yl)-*N*-hydroxy-3-oxo-propionamide (54; Method C): Yellow oil; yield 21% after purification by thick layer chromatography; purity 95%; ¹H NMR (DMSO-*d*₆) δ 0.73–1.07 (m, 2H), 1.32–1.55 (m, 2H), 1.60–1.75 (m, 1H), 2.27–2.50 (m, 3H), 2.73–2.96 (m, 2H), 3.01–3.11 (m, 1H), 3.63–3.72 (m, 1H), 3.83–3.94 (m, 1H), 4.31 (d, *J* = 12.7 Hz, 1H), 7.09–7.27 (m, 10H), 8.87 (s, 0.55 OH), 8.92 (s, 0.45 OH), 10.43 (0.55 CONHO), 10.54 (s, 0.45 CONHO); *t*_{R(LCMS)} 5.46 min; MS (MH)⁺ *m/z* 367.

2-Benzyl-3-(4-benzyl-piperazin-1-yl)-*N*-hydroxy-3-oxo-propionamide (55; Method C): Orange powder; yield 72%; purity 96%; ¹H NMR (DMSO-*d*₆) δ 2.56–2.66 (m, 2H), 2.99 (d, *J* = 6.3 Hz, 2H), 3.05–3.23 (m, 6H), 3.57–3.69 (m, 2H), 3.73–3.79 (m, 1H), 7.19–7.43 (m, 10H), 8.95 (s, OH), 10.56 (s, CONHO); *t*_{R(LCMS)} 3.16 min; MS (MH)⁺ *m/z* 368.

2-Benzyl-3-(3,4-dihydro-1H-isoquinolin-2-yl)-N-hydroxy-3-oxo-propionamide (56; Method A): Beige powder; yield 46%; purity 100%; ^1H NMR (DMSO- d_6) δ 2.67–2.79 (m, 2H), 3.00–3.08 (m, 2.5H), 3.56–3.79 (m, 2.5H), 3.28–3.35 (m, 0.5H), 4.44–4.50 (m, 0.5H), 4.61–4.69 (m, 1H), 7.10–7.23 (m, 9H), 8.95 (s, OH), 10.62 (s, CONHO); $t_{\text{R(LCMS)}}$ 4.53 min; MS (MH) $^+$ m/z 325; mp 137–142 °C.

2-Benzyl-N-(4-fluoro-benzyl)-N'-hydroxy-malonamide (57; Method C): White powder; yield 88%; purity 100%; ^1H NMR (DMSO- d_6) δ 2.96–3.10 (m, 2H), 3.35–3.40 (m, 1H), 4.16 (dd, $J = 15$, $J = 5.7$ Hz, 1H), 4.27 (dd, $J = 15$, $J = 6$ Hz, 1H), 7.04–7.27 (m, 9H), 8.40 (t, $J = 5.6$ Hz, NHCO), 8.93 (s, OH), 10.58 (s, CONHO); ^{13}C NMR (DMSO- d_6) δ 35.0, 42.1, 52.5, 115.5 (d, $J_{\text{CF}} = 21.1$ Hz), 126.8, 128.8, 129.4, 129.5 (d, $J_{\text{CF}} = 8.4$ Hz), 136.0 (d, $J_{\text{CF}} = 2.3$ Hz), 139.6, 161.7 (d, $J_{\text{CF}} = 240.4$ Hz), 166.3, 168.9; $t_{\text{R(LCMS)}}$ 4.31 min; MS (MH) $^+$ m/z 317; mp 193–194 °C.

2-Benzyl-N-(4-chloro-benzyl)-N'-hydroxy-malonamide (58; Method C): White powder; yield 90%; purity 97%; ^1H NMR (DMSO- d_6) δ 3.00–3.08 (m, 2H), 3.30 (t, $J = 7.35$ Hz, 1H), 4.19 (dd, $J = 4.8$ Hz, $J = 14.7$ Hz, 1H), 4.26 (dd, $J = 6.3$ Hz, $J = 14.4$ Hz, 1H), 7.10–7.32 (m, 9H), 8.26–8.28 (m, NHCO), 10.46 (s, CONHO); ^{13}C NMR (DMSO- d_6) δ 35.1, 42.0, 52.8, 126.7, 128.5, 128.6, 129.2, 129.3, 131.6, 138.8, 139.3, 166.2, 168.7; $t_{\text{R(LCMS)}}$ 4.80 min; MS (MH) $^+$ m/z 333; mp 198–200 °C.

2-Benzyl-N-hydroxy-N'-(2-methyl-benzyl)-malonamide (59; Method C): White powder; yield 85%; purity 97%; ^1H NMR (DMSO- d_6) δ 2.18 (s, 3H), 3.02–3.06 (m, 2H), 3.32 (t, $J = 7.5$ Hz, 1H), 4.14–4.23 (m, 2H), 6.99–7.25 (m, 9H), 8.05 (t, $J = 5.4$ Hz, NHCO), 8.95 (s, OH), 10.42 (s, CONHO); ^{13}C NMR (DMSO- d_6) δ 19.0, 35.1, 41.0, 52.7, 126.1, 126.6, 127.3, 127.9, 128.6, 129.3, 130.3, 136.1, 137.0, 139.4, 166.3, 168.4; $t_{\text{R(LCMS)}}$ 4.53 min; MS (MH) $^+$ m/z 313; mp 191–193 °C.

2-Benzyl-N-hydroxy-N'-naphthalen-1-ylmethyl-malonamide (60; Method A): Beige powder; yield 25%; purity 99%; ^1H NMR (DMSO- d_6) δ 3.03 (dd, $J = 7.9$ Hz, $J = 13.6$ Hz, 1H), 3.11 (dd, $J = 7.6$ Hz, $J = 13.6$ Hz, 1H), 3.32–3.35 (m, 1H), 4.62 (dd, $J = 15.3$, $J = 5.1$ Hz, 1H), 4.77 (dd, $J = 15.3$, $J = 6.0$ Hz, 1H), 7.19–7.25 (m, 6H), 7.39 (t, $J = 7.6$ Hz, 1H), 7.51–7.54 (m, 2H), 7.83 (d, $J = 8.1$ Hz, 1H), 7.92–7.99 (m, 2H), 8.27 (t, $J = 5.4$ Hz, NHCO), 8.95 (s, OH), 10.44 (s, CONHO); ^{13}C NMR (DMSO- d_6) δ 35.1, 40.1, 52.7, 123.8, 125.5, 125.8, 126.2, 126.6, 126.7, 127.9, 128.6, 128.9, 129.3, 131.2, 133.7, 134.6, 139.4, 166.2, 168.6; $t_{\text{R(LCMS)}}$ 4.89 min; MS (MH) $^+$ m/z 349; mp 156–159 °C.

2-Benzyl-N-hydroxy-N'-(3-phenoxy-benzyl)-malonamide (61; Method B): White powder; yield 64%; purity 99%; ^1H NMR (DMSO- d_6) δ 3.01 (d, $J = 7.5$ Hz, 2H), 3.29 (dd, $J = 4.2$ Hz, $J = 7.8$ Hz, 1H), 4.18 (dd, $J = 5.7$ Hz, $J = 15.3$ Hz, 1H), 4.29 (dd, $J = 5.7$ Hz, $J = 15.3$ Hz, 1H), 6.83–6.90 (m, 3H), 6.99 (d, $J = 7.8$ Hz, 2H), 7.10–7.30 (m, 7H), 7.39 (t, $J = 7.8$ Hz, 2H), 8.26 (t, $J = 6$ Hz, NHCO), 8.94 (s, 1H, OH), 10.46 (s, 1H, CONHO); ^{13}C NMR (DMSO- d_6) δ 35.1, 42.4, 52.8, 117.3, 117.8, 119.0, 122.6, 123.8, 126.7, 128.6, 129.2, 130.3, 130.5, 139.4, 142.1, 157.0, 157.1, 166.2, 168.7; $t_{\text{R(LCMS)}}$ 5.45 min; MS (MH) $^+$ m/z 391.

2-Benzyl-N-biphenyl-3-ylmethyl-N'-hydroxy-malonamide (62; Method B): White powder; yield 71%; purity 99%; ^1H NMR (DMSO- d_6) δ 3.03–3.09 (m, 2H), 3.28–3.32 (m, 1H), 4.28 (dd, $J = 5.8$ Hz, $J = 15.3$ Hz, 1H), 4.37 (dd, $J = 6.0$ Hz, $J = 15.0$ Hz, 1H), 7.10–7.22 (m, 6H), 7.34–7.39 (m, 2H), 7.45–7.52 (m, 4H), 7.62–7.65 (m, 2H), 8.29 (t, $J = 5.4$ Hz, NHCO), 8.94 (s, 1H, OH), 10.48 (s, 1H, CONHO); $t_{\text{R(LCMS)}}$ 5.43 min; MS (MH) $^+$ m/z 375.

2-Benzyl-N-(2,2-diphenyl-ethyl)-N'-hydroxy-malonamide (63; Method B): White powder; yield 50%; purity 98%; ^1H NMR (DMSO- d_6) δ 2.84 (d, $J = 7.5$ Hz, 2H), 3.11 (t, $J = 7.2$ Hz, 1H), 3.59–3.78 (m, 2H), 4.11 (t, $J = 7.8$ Hz, 1H), 7.06–7.29 (m, 15H), 7.69 (t, $J = 5.4$ Hz, 1H, NHCO), 8.91 (s, 1H, OH), 9.85 (s, 1H, CONHO); $t_{\text{R(LCMS)}}$ 5.49 min; MS (MH) $^+$ m/z 389.

2-[1-Phenyl-meth-(Z)-ylidene]-malonic Acid Monoethyl Ester (65). In a round-bottom flask containing a solution of LiOH (1.05 g; 25 mmol; 1 equiv) dissolved in THF (50 mL) and water (50 mL) was added diethyl benzylidene malonate (5.60 mL; 25 mmol; 1

equiv). The reaction mixture was stirred 4 h at room temperature. THF was evaporated under reduced pressure. A solution of NaHCO₃ 5% was added, and the remaining diethyl ester was extracted with DCM. The aqueous phase was then acidified to pH = 1 with HCl, and the expected product was extracted three times with DCM. The organic phases were joined, dried over MgSO₄, and evaporated under reduced pressure to give 2-[1-phenyl-meth-(Z)-ylidene]-malonic acid monoethyl ester (65) as a white powder. The configuration of this acid was determined by nondecoupled ^{13}C NMR experiment (see Supporting Information). Yield 85%; purity 98%; ^1H NMR (DMSO- d_6) δ 1.20 (t, $J = 7.2$ Hz, 3H), 4.26 (q, $J = 7.2$ Hz, 2H), 7.43–7.51 (m, 5H), 7.66 (s, 1H), 13.35 (s, 1H, OH); MS (MH) $^+$ m/z 221.

N-(4-Fluoro-benzyl)-N'-hydroxy-2-[1-phenyl-meth-(Z)-ylidene]-malonamide (66). Acid (65; 2.225 g; 10.1 mmol; 1 equiv) was dissolved in DCM (25 mL) with catalytic DMF (75 μL). The mixture was cooled at 0 °C (ice bath), and oxalyl chloride (1.041 mL; 12.1 mmol; 1.2 equiv) was added dropwise. The reaction mixture was stirred 45 min at 0 °C and then evaporated under reduced pressure. The residue was dissolved in DCM (25 mL) and cooled at 0 °C. DIEA (5 mL; 30 mmol; 3 equiv) was added and then *O*-trityl-hydroxylamine (2.365 g; 8.6 mmol; 0.85 equiv) was added. The reaction mixture was stirred 3 h at room temperature. The organic phase was washed with NaHCO₃ 5%, dried over MgSO₄, and evaporated under reduced pressure. A minimum of DCM was added and trituration with petroleum ether allowed (Z)-3-phenyl-2-trityloxycarbonyl-acrylic acid ethyl ester as a white powder. The configuration of this compound was determined by ROESY NMR experiment. Yield 45%; purity 95%; ^1H NMR (DMSO- d_6) δ 1.19 (t, $J = 7.2$ Hz, 3H), 4.13 (q, $J = 7.2$ Hz, 2H), 7.21–7.35 (m, 20H), 7.51 (s, 1H), 10.37 (s, 1H, NH); MS (MNa) $^+$ m/z 500. A total of 900 mg (1.9 mmol; 1 equiv) of ester was dissolved in 20 mL of a mixture of THF and water (1/1). A total of 320 mg of LiOH (7.6 mmol; 4 equiv) was added, and the mixture was stirred overnight at room temperature. THF was evaporated under reduced pressure. The aqueous phase was then acidified to pH = 6 with HCl 1 N, and the expected product was extracted four times with DCM. The organic phases were joined, dried over MgSO₄, and evaporated under reduced pressure. As this stage, the double bond is isomerized to give (*E*)-3-phenyl-2-trityloxycarbonyl-acrylic acid as a white powder. The configuration of this acid was determined by nondecoupled ^{13}C NMR experiment. Yield 85%; purity 95%; ^1H NMR (CD₂Cl₂) δ 7.16–7.39 (m, 20H), 7.90 (s, 1H); MS (MH) $^-$ m/z 448. This acid (297 mg; 0.66 mmol; 1 equiv) was dissolved in DCM (7 mL), and TEA (102 μL ; 0.73 mmol; 1.1 equiv) was added. The mixture was cooled at 0 °C (ice bath) and ethylchloroformate (70 μL ; 0.73 mmol; 1.1 equiv) was added dropwise. The reaction mixture was stirred 30 min at 0 °C and then 4-fluorobenzylamine (84 μL ; 0.73 mmol; 1.1 equiv) was added. The organic layer was stirred 1 h at room temperature and then evaporated. The crude product was dissolved in ethyl acetate, washed twice with aq. NaHCO₃ 5%, once with water, and once with aq. NaCl, dried over MgSO₄, filtered, and evaporated. The product was purified by thick layer chromatography (DCM 100%) then precipitated in petroleum ether to give a white powder. Yield 20%; purity 95%; MS (MH) $^-$ m/z 555. The protected hydroxamic acid (64 mg; 0.11 mmol) was dissolved in TFA 2%/DCM (0.03 M), and triisopropylsilane was added drop by drop until the yellow color disappeared. The reaction mixture was stirred 5 min at room temperature, solvents were removed under reduced pressure, and the residue was washed with petroleum ether to give (66) as a white powder. The configuration of this compound was determined by ROESY NMR experiment (see Supporting Information). Yield 96%; purity 99%; NMR ^1H NMR (DMSO- d_6) δ 4.37 (d, $J = 6.0$ Hz, 2H), 7.12–7.18 (m, 2H), 7.32–7.40 (m, 5H), 7.43 (s, 1H), 7.51–7.54 (m, 2H), 8.26 (t, $J = 6.0$ Hz, NHCO), 9.13 (s, OH), 11.01 (s, CONHO); ^{13}C NMR (DMSO- d_6) δ 42.6, 115.6 (d, $J_{\text{CF}} = 21$ Hz), 129.3, 129.5, 129.9, 130.1, 130.6, 134.2, 136.2, 137.3, 161.8 (d, $J_{\text{CF}} = 246$ Hz), 163.5, 164.6; $t_{\text{R(LCMS)}}$ 4.23 min; MS (MH) $^+$ m/z 315.

***N*-Hydroxy-*N'*-(4-phenyl-butyl)-2-[1-phenyl-meth-(*Z*)-ylidene]-malonamide (67).** (*E*)-3-Phenyl-2-trityloxycarbonyl-acrylic acid (see synthesis of **66**; 180 mg; 0.4 mmol; 1 equiv) was dissolved in DCM (4 mL) and TEA (62 μ L; 0.44 mmol; 1.1 equiv) was added. The mixture was cooled at 0 °C (ice bath) and ethylchloroformate (42 μ L; 0.44 mmol; 1.1 equiv) was added dropwise. The reaction mixture was stirred 30 min at 0 °C, and then phenylbutylamine (70 μ L; 0.44 mmol; 1.1 equiv) was added. The organic layer was stirred 1 h at room temperature and then evaporated. The crude product was dissolved in ethyl acetate, washed twice with aq. NaHCO₃ 5%, once with water, and once with aq. NaCl, dried over MgSO₄, filtered, and evaporated. The product was purified by thick layer chromatography (DCM/MeOH 98/2) and then precipitated in petroleum ether to give a white powder. Yield 20%; purity 99%; MS (MNa)⁺ *m/z* 603. The protected hydroxamic acid (46 mg; 0.08 mmol) was dissolved in TFA 2%/DCM (0.03 M), and triisopropylsilane was added drop by drop until the yellow color disappeared. The reaction mixture was stirred 5 min at room temperature, solvents were removed under reduced pressure, and the residue was washed with petroleum ether to give (**67**) as a white powder. The configuration of this compound was assessed by ROESY NMR experiment. Yield 89%; purity 99%; ¹H NMR (DMSO-*d*₆) δ 1.47–1.61 (m, 4H), 2.59 (t, *J* = 7.2 Hz, 2H), 3.17–3.23 (m, 2H), 7.14–7.30 (m, 5H), 7.36 (s, 1H), 7.37–7.40 (m, 3H), 7.48–7.52 (m, 2H), 7.71 (t, *J* = 5.7 Hz, NHCO), 9.13 (br s, OH), 10.95 (s, CONHO); ¹³C NMR (DMSO-*d*₆) δ 28.8, 29.2, 35.3, 39.3, 126.1, 128.7, 128.8, 129.1, 129.8, 129.9, 130.7, 134.2, 136.6, 142.6, 163.6, 164.3; *t*_{R(LCMS)} 5.07 min; MS (MH)⁺ *m/z* 337.

***N*-(4-Fluoro-benzyl)-*N'*-hydroxy-2-[1-phenyl-meth-(*E*)-ylidene]-malonamide (68).** Acid (**65**; 110 mg; 0.5 mmol; 1 equiv) was dissolved in DCM (5 mL), and TEA (77 μ L; 0.55 mmol; 1.1 equiv) was added. The mixture was cooled at 0 °C (ice bath), and ethylchloroformate (53 μ L; 0.55 mmol; 1.1 equiv) was added dropwise. The reaction mixture was stirred 30 min at 0 °C, and then 4-fluorobenzylamine (57 μ L; 0.5 mmol; 1 equiv) was added. The organic layer was stirred 1 h at room temperature and then evaporated. The crude product was dissolved in ethyl acetate, washed twice with water and once with aq. NaCl, dried over MgSO₄, filtered, and evaporated. At this stage, the double bond is isomerized to give (*E*)-2-(4-fluoro-benzylcarbamoyl)-3-phenyl-acrylic acid ethyl ester. Yield 95%; purity 95%; ¹H NMR (DMSO-*d*₆) δ 1.24 (t, *J* = 7.2 Hz, 3H), 4.22 (q, *J* = 7.2 Hz, 2H), 4.37 (d, *J* = 6 Hz, 2H), 7.12–7.18 (m, 2H), 7.31–7.44 (m, 5H), 7.52–7.55 (m, 2H), 7.58 (s, 1H), 8.99 (t, *J* = 6 Hz, NH); MS (MH)⁺ *m/z* 328. A total of 147 mg (0.45 mmol; 1 equiv) of ester was dissolved in 5 mL of a mixture of THF and water (1/1). A total of 76 mg of LiOH (1.8 mmol; 4 equiv) was added, and the mixture was stirred overnight at room temperature. THF was evaporated under reduced pressure. The aqueous phase was washed three times with DCM and then acidified to pH = 1 with HCl. The expected product was extracted three times with DCM. The organic phases were joined, dried over MgSO₄, evaporated under reduced pressure, and then precipitated in petroleum ether to give (*E*)-2-(4-fluoro-benzylcarbamoyl)-3-phenyl-acrylic acid as a white powder. Yield 75%; purity 95%; ¹H NMR (DMSO-*d*₆) δ 4.34 (d, *J* = 6 Hz, 2H), 7.10–7.15 (m, 2H), 7.26–7.40 (m, 5H), 7.46–7.49 (m, 2H), 7.50 (s, 1H), 8.90 (t, *J* = 6 Hz, NH), 12.43 (s, OH); MS (MH)⁺ *m/z* 298. The previous synthesized acid (90 mg; 0.3 mmol; 1 equiv) was dissolved in DCM (3 mL), and TEA (46 μ L; 0.33 mmol; 1.1 equiv) was added. The mixture was cooled at 0 °C (ice bath), and ethylchloroformate (31 μ L; 0.33 mmol; 1.1 equiv) was added dropwise. The reaction mixture was stirred for 30 min at 0 °C, and then *O*-tritylhydroxylamine (70 mg; 0.25 mmol; 0.85 equiv) was added. The organic layer was stirred 1 h at room temperature and then evaporated. The crude product was dissolved in DCM, washed three times with aq. NaHCO₃ 5%, once with water and once with aq. NaCl, dried over MgSO₄, filtered, and evaporated. The product was purified by thick layer chromatography (DCM/MeOH 99/1) to give a white powder. Yield 35%; purity 95%; MS (MH)⁺ *m/z* 555. The protected hydroxamic acid (20 mg; 0.036 mmol) was dissolved in TFA 2%/DCM (0.03 M), and triisopropylsilane was added drop

by drop until the yellow color disappeared. The reaction mixture was stirred 5 min at room temperature, solvents were removed under reduced pressure, and the residue was washed with petroleum ether to give (**68**) as a white powder. (See Supporting Information for stereochemical assignment). Yield 70%; purity 99%; ¹H NMR (DMSO-*d*₆) δ 4.30 (d, *J* = 6.0 Hz, 2H), 7.08–7.37 (m, 10H), 8.86 (t, *J* = 6.0 Hz, NHCO), 9.08 (br s, OH), 10.70 (br s, CONHO); ¹³C NMR (DMSO-*d*₆) δ 42.3, 115.3 (d, *J*_{CF} = 20 Hz), 128.9, 129.5, 129.6, 129.8, 130.3 (d, *J*_{CF} = 12 Hz), 132.0, 134.3, 135.2, 161.4 (d, *J*_{CF} = 225 Hz), 163.3, 166.2; *t*_{R(LCMS)} 4.41 min; MS (MH)⁺ *m/z* 315.

2-(2-Nitro-benzylidene)-malonic Acid Diethyl Ester (69). To a solution of diethylmalonic ester (3.843 mL; 27 mmol; 1.2 equiv), acetic acid (519 μ L; 9 mmol; 0.4 equiv), and piperidine (265 μ L; 2.7 mmol; 0.12 equiv) in benzene (60 mL) was added 2-nitrobenzaldehyde (3.40 g; 22.5 mmol; 1 equiv). The reaction mixture was refluxed for 72 h and then evaporated. The crude product was dissolved in ethyl acetate, washed four times with aq. NaHCO₃ 5%, and once with aq. NaCl, dried over MgSO₄, filtered, and evaporated. The product was purified over silica gel (BP SUP 110 g Silice Flashsmart) with cyclohexane/AcOEt (100/0 to 95/5) to give **69** as a colorless oil. Yield 12%; purity 99%; ¹H NMR (DMSO-*d*₆) δ 0.95 (t, *J* = 7.2 Hz, 3H), 1.26 (t, *J* = 7.2 Hz, 3H), 4.04 (q, *J* = 7.2 Hz, 2H), 4.28 (q, *J* = 7.2 Hz, 2H), 7.43 (dt, *J* = 7.5 Hz, *J* = 0.9 Hz, 1H), 7.69–7.74 (m, 1H), 7.83 (td, *J* = 7.5 Hz, *J* = 1.5 Hz, 1H), 8.17 (s, 1H), 8.24 (dd, *J* = 1.2 Hz, *J* = 8.1 Hz, 1H); MS (MH)⁺ *m/z* 294, (MNa)⁺ *m/z* 316.

1-Hydroxy-2-oxo-1,2-dihydro-quinoline-3-carboxylic Acid Ethyl Ester (70). Compound **69** (307 mg, 1.05 mmol) was dissolved in acetic acid (5 mL), and PtO₂ (5 mg) was added. The reaction mixture was stirred 24 h at room temperature under hydrogen, then filtered over celite, and washed with methanol. The solvents were evaporated under reduced pressure. The product was purified by thick layer chromatography (DCM/TEA 9/1) to give **70** as a beige powder. Yield 55%; purity 99%; ¹H NMR (CD₂Cl₂) δ 1.43 (t, *J* = 7.2 Hz, 3H), 4.43 (q, *J* = 7.2 Hz, 2H), 7.37–7.42 (m, 1H), 7.79–7.83 (m, 3H), 8.59 (s, 1H); MS (MH)⁺ *m/z* 234.

1-Hydroxy-2-oxo-1,2-dihydro-quinoline-3-carboxylic Acid 4-Fluoro-benzylamide (71). Compound **70** (37 mg; 0.16 mmol) was dissolved in 4-fluorobenzylamine (2 mL), and the reaction mixture was heated at 60 °C for 4 h, and then cooled at room temperature. Ethyl acetate was added, and the organic layer was washed four times with HCl 1 N, once with water, once with brine, dried over MgSO₄, filtered, and evaporated. The residue was precipitated in DCM and filtered to give **71** as a beige powder. Yield 70%; purity 99%; ¹H NMR (DMSO-*d*₆) δ 4.58 (d, *J* = 6.0 Hz, 2H), 7.14–7.20 (m, 2H), 7.38–7.41 (m, 3H), 7.76–7.81 (m, 2H), 8.05 (d, *J* = 7.5 Hz, 1H), 8.85 (s, 1H), 10.06 (t, *J* = 6.0 Hz, NH), 11.82 (s, 1H, OH); ¹³C NMR (DMSO-*d*₆) δ 42.5, 113.2, 115.8 (d, *J*_{CF} = 21 Hz), 118.4, 121.9, 123.9, 130.0 (d, *J*_{CF} = 8 Hz), 130.8, 134.0, 135.9, 139.7, 141.4, 158.1, 161.9 (d, *J*_{CF} = 240 Hz), 163.1; *t*_{R(LCMS)} 5.10 min; MS (MH)⁺ *m/z* 313.

1-Hydroxy-2-oxo-1,2-dihydro-quinoline-3-carboxylic Acid (4-Phenyl-butyl)-amide (72). Compound **70** (47 mg; 0.2 mmol) was dissolved in phenylbutylamine (2 mL) and the reaction mixture was heated at 60 °C for 4h, then cooled at room temperature. Ethyl acetate was added, and the organic layer was washed four times with HCl 1 N, once with water, once with brine, dried over MgSO₄, filtered, and evaporated. The residue was precipitated in DCM and filtered to give **72** as a beige powder. Yield 87%; purity 99%; ¹H NMR (DMSO-*d*₆) δ 1.57–1.63 (m, 4H), 2.57–2.64 (m, 2H), 3.38–3.43 (m, 2H), 7.14–7.29 (m, 5H), 7.36–7.41 (m, 1H), 7.76–7.81 (m, 2H), 8.04 (d, *J* = 7.5 Hz, 1H), 8.82 (s, 1H), 9.70 (t, *J* = 5.4 Hz, NH), 11.81 (s, 1H, OH); ¹³C NMR (DMSO-*d*₆) δ 29.0, 29.2, 32.3, 39.1, 113.2, 118.3, 121.8, 123.9, 126.3, 128.8, 128.9, 130.7, 134.0, 139.7, 141.1, 142.6, 158.0, 162.7; *t*_{R(LCMS)} 6.01 min; MS (MH)⁺ *m/z* 337.

Acknowledgment. The authors would like to thank Professors André Tartar and H el ene Gras for fruitful discussions. We are grateful to the institutions that support our laboratory

(Inserm, Université de Lille2 and Institut Pasteur de Lille). Marion Flipo received a grant from CNRS and Région Nord-Pas-de-Calais. This work was specifically funded by Région Nord-Pas-de-Calais and EC. NMR spectra were recorded in the Laboratoire d'Application RMN (LARMN) at Université de Lille2, Faculté des Sciences Pharmaceutiques de Lille. Data management was performed using Pipeline Pilot from Scitegic.

Supporting Information Available: Screening results for the whole library, spectral NMR, and other analytical data that support configuration assignments of **65**, **66**, and **68**. This material is available free of charge via the Internet at <http://pubs.acs.org>.

References

- 1.3 million deaths in 2004 (World Health Organization Global report 2004, Geneva, 2004), 3 billion people at risk in 2005 (World Malaria Report 2005 from Roll Back Malaria Partnership, available at www.rbm.who.int/wmr2005/).
- Malenga, G.; Palmer, A.; Staedke, S.; Kazadi, W.; Mutabingwa, T.; Ansah, E.; Barnes, K. I.; Whitty, C. J. Antimalarial treatment with artemisinin combination therapy in Africa. *Br. Med. J.* **2005**, *331*, 706–707.
- Edwards, G.; Biagini, G. A. Resisting resistance: Dealing with the irrepressible problem of malaria. *Br. J. Clin. Pharmacol.* **2006**, *61*, 690–693.
- Bloland, P. B. *Drug resistance in malaria*, World Health Organization report; World Health Organization: Geneva, Switzerland, 2001.
- Phillips, M.; Phillips-Howard, P. A. Economic implications of resistance to antimalarial drugs. *Pharmacoeconomics* **1996**, *10*, 225–238.
- Greenwood, B. M.; Bojang, K.; Whitty, C. M.; Targett, G. A. Malaria. *Lancet* **2005**, *365*, 1487–1498.
- Plasmodium* genomics special issue. *Nature* **2002**, special issue, October 3, 2002.
- Yeh, I.; Altman, R. B. Drug Targets for *Plasmodium falciparum*: A post-genomic review/survey. *Mini-Rev. Med. Chem.* **2006**, *6*, 177–202.
- Woster, P. M. New Therapies for Malaria. In *Annu. Rep. Med. Chem.*; Doherty, A. M., Ed.; Academic Press: New York, 2003; Vol. 38, pp 203–211.
- For a review on chemotherapy research: Wiesner, J.; Ortmann, R.; Jomaa, H.; Schitser, M. New antimalarial drugs. *Angew. Chem., Int. Ed.* **2003**, *42*, 5274–5293.
- O'Donnell, R. A.; Blackman, M. J. The role of malaria merozoite proteases in red blood cell invasion. *Curr. Opin. Microbiol.* **2005**, *8*, 422–427.
- Blackman, M. J. Proteases involved in erythrocyte invasion by the malaria parasite: function and potential as chemotherapeutic targets. *Curr. Drug Targets* **2000**, *1*, 59–83.
- Blackman, M. J. Proteases in host cell invasion by the malaria parasite. *Cell Microbiol.* **2004**, *6*, 893–903.
- Rosenthal, P. J. Hydrolysis of erythrocyte proteins by proteases of malaria parasites. *Curr. Opin. Hematol.* **2002**, *9*, 140–145.
- Wu, Y.; Wang, X.; Liu, X.; Wang, Y. Data-Mining Approaches Reveal Hidden Families of Proteases in the Genome of Malaria Parasite. *Genome Res.* **2003**, *13*, 601–616.
- Klemba, M.; Gluzman, I.; Goldberg, D. E. A *Plasmodium falciparum* Dipeptidyl Aminopeptidase I Participates in Vacuolar Hemoglobin Degradation. *J. Biol. Chem.* **2004**, *279*, 43000–43007.
- Withers-Martinez, C.; Jean, L.; Blackman, M. J. Subtilisin-like proteases of the malaria parasite. *Mol. Microbiol.* **2004**, *53*, 55–63.
- Ersmark, K.; Feierberg, I.; Bjelic, S.; Hamelink, E.; Hackett, F.; Blackman, M. J.; Hulten, J.; Samuelsson, B.; Aqvist, J.; Hallberg, A. Potent inhibitors of the *Plasmodium falciparum* enzymes plasmeprin I and II devoid of cathepsin D inhibitory activity. *J. Med. Chem.* **2004**, *47*, 110–122.
- Ersmark, K.; Nervall, M.; Hamelink, E.; Janka, L. K.; Clemente, J. C.; Dunn, B. M.; Blackman, M. J.; Samuelsson, B.; Aqvist, J.; Hallberg, A. Synthesis of malarial plasmeprin inhibitors and prediction of binding modes by molecular dynamics simulations. *J. Med. Chem.* **2005**, *48*, 6090–6106.
- Ersmark, K.; Nervall, M.; Gutierrez-de-Teran, H.; Hamelink, E.; Janka, L. K.; Clemente, J. C.; Dunn, B. M.; Gogoll, A.; Samuelsson, B.; Qvist, J.; Hallberg, A. Macrocyclic inhibitors of the malarial aspartic proteases plasmeprin I, II, and IV. *Bioorg. Med. Chem.* **2006**, *14*, 2197–2208.
- Nezami, A.; Kimura, T.; Hidaka, K.; Kiso, A.; Liu, J.; Kiso, Y.; Goldberg, D. E.; Freire, E. High-affinity inhibition of a family of *Plasmodium falciparum* proteases by a designed adaptive inhibitor. *Biochemistry* **2003**, *42*, 8459–8464.
- Andrews, K. T.; Fairlie, D. P.; Madala, P. K.; Ray, J.; Wyatt, D. M.; Hilton, P. M.; Melville, L. A.; Beattie, L.; Gardiner, D. L.; Reid, R. C.; Stoermer, M. J.; Skinner-Adams, T.; Berry, C.; McCarthy, J. S. Potencies of human immunodeficiency virus protease inhibitors *in vitro* against *Plasmodium falciparum* and *in vivo* against murine malaria. *Antimicrob. Agents Chemother.* **2006**, *50*, 639–648.
- Desai, P. V.; Patny, A.; Sabnis, Y.; Tekwani, B.; Gut, J.; Rosenthal, P.; Srivastava, A.; Avery, M. Identification of novel parasitic cysteine protease inhibitors using virtual screening. 1. The ChemBridge database. *J. Med. Chem.* **2004**, *47*, 6609–6615.
- Desai, P. V.; Patny, A.; Gut, J.; Rosenthal, P. J.; Tekwani, B.; Srivastava, A.; Avery, M. Identification of novel parasitic cysteine protease inhibitors by use of virtual screening. 2. The available chemical directory. *J. Med. Chem.* **2006**, *49*, 1576–1584.
- Lee, B. J.; Singh, A.; Chiang, P.; Kemp, S. J.; Goldman, E. A.; Weinhouse, M. I.; Vlasuk, G. P.; Rosenthal, P. J. Antimalarial activities of novel synthetic cysteine protease inhibitors. *Antimicrob. Agents Chemother.* **2003**, *47*, 3810–3814.
- Batra, S.; Sabnis, Y. A.; Rosenthal, P. J.; Avery, M. A. Structure-based approach to falcipain-2 inhibitors: Synthesis and biological evaluation of 1,6,7-trisubstituted dihydroisoquinolines and isoquinolines. *Bioorg. Med. Chem.* **2003**, *11*, 2293–2299.
- Greenbaum, D. C.; Mackey, Z.; Hansell, E.; Doyle, P.; Gut, J.; Caffrey, C. R.; Lehrman, J.; Rosenthal, P. J.; McKerrow, J. H.; Chibale, K. Synthesis and structure–activity relationships of parasiticidal thiosemicarbazone cysteine protease inhibitors against *Plasmodium falciparum*, *Trypanosoma brucei*, and *Trypanosoma cruzi*. *J. Med. Chem.* **2004**, *47*, 3212–3219.
- Verhelst, S. H.; Witte, M. D.; Arastu-Kapur, S.; Fonovic, M.; Bogoyo, M. Novel aza peptide inhibitors and active-site probes of papain-family cysteine proteases. *ChemBioChem* **2006**, *7*, 943–950.
- Murata, C. E.; Goldberg, D. E. *Plasmodium falciparum* falcylisin. *J. Biol. Chem.* **2003**, *278*, 38022–38028.
- Gardiner, D. L.; Trenholme, K. R.; Skinner-Adams, T. S.; Stack, C. M.; Dalton, J. P. Overexpression of leucyl aminopeptidase in *Plasmodium falciparum* parasites. *J. Biol. Chem.* **2006**, *281*, 1741–1745.
- Florent, I.; Derhy, Z.; Allary, M.; Monsigny, M.; Mayer, R.; Schrevel, J. A *Plasmodium falciparum* aminopeptidase gene belonging to the M1 family of zinc-metalloproteases is expressed in erythrocytic stages. *Mol. Biochem. Parasitol.* **1998**, *97*, 149–160.
- Chen, X.; Chong, C. R.; Shi, L.; Yoshimoto, T.; Sullivan, D. J.; Liu, J. O. Inhibitors of *Plasmodium falciparum* methionine aminopeptidase 1b possess antimalarial activity. *Proc. Natl. Acad. Sci. U.S.A.* **2006**, *103*, 14548–14553.
- Ponpuak, M.; Klemba, M.; Park, M.; Gluzman, I. Y.; Lamppa, G. K.; Golberg, D. E. A role for falcylisin in transit peptide degradation in the *Plasmodium falciparum* apicoplast. *Mol. Microbiol.* **2006**, *63*, 314–334.
- PfA-M1 is referenced as MAL8P1.56 in PlasmoDB (<http://plasmodb.org>).
- Allary, M.; Schrevel, J.; Florent, I. Properties, stage-dependent expression and localization of *Plasmodium falciparum* M1 family zinc-aminopeptidase. *Parasitology* **2002**, *125*, 1–10.
- Kitjaroentharn, A.; Suthiphongchai, T.; Wilairat, P. Effect of metalloprotease inhibitors on invasion of red blood cell by *Plasmodium falciparum*. *Acta Trop.* **2006**, *97*, 5–9.
- Deprez-Poulain, R.; Melnyk, P. 1,4-bis(3-aminopropyl)piperazine libraries: from the discovery of classical chloroquine-like antimalarials to the identification of new targets. *Comb. Chem. High Throughput Screening* **2005**, *8*, 39–48.
- Flipo, M.; Florent, I.; Grellier, P.; Sergheraert, C.; Deprez-Poulain, R. Design, synthesis and antimalarial activity of novel, quinoline-based, zinc metallo-aminopeptidase inhibitors. *Bioorg. Med. Chem. Lett.* **2003**, *13*, 2659–2662.
- Flipo, M.; Beghyn, T.; Charton, J.; Leroux, V. A.; Deprez, B. P.; Deprez-Poulain, R. F. A library of novel hydroxamic acids targeting the metallo-protease family: Design, parallel synthesis and screening. *Bioorg. Med. Chem.* **2007**, *15*, 63–76.
- Zhang, J. H.; Chung, T. D.; Oldenburg, K. R. A simple statistical parameter for use in evaluation and validation of high-throughput screening assays. *J. Biomol. Screening* **1999**, *4*, 67–73.
- Sicker, D.; Rabe, A.; Zakrzewski, A.; Mann, G. Synthese substituierter *N*-hydroxylactame, lactame, chinolin-*N*-oxide und chinoline durch katalysierte reduktive cyclisierung von 2-nitrocinnamoyl-verbindungen mit Wasserstoff/Platinschwarz. *J. Prakt. Chem.* **1987**, *329*, 1063–1070.
- ABS was calculated using an in-house PipelinePilot™ (from Scitegic) protocol based on the following publication: Martin, Y. C. A bioavailability score. *J. Med. Chem.* **2005**, *48*, 3164–3170. This article underlines the fact that the polar surface area (PSA) and the rule-of-five govern bioavailability of anionic compounds and of neutral, zwitterionic, or cationic compounds, respectively.

- (43) Hadjuk, P. J.; Shuker, S. B.; Nettesheim, D. G.; Craig, R.; Augeri, D. J.; Betebenner, D.; Albert, D. H.; Guo, Y.; Meadows, R. P.; Xu, L.; Michaelides, M.; Davidsen, S. K.; Fesik, S. W. NMR-based modification of matrix metalloproteinase inhibitors with improved bioavailability. *J. Med. Chem.* **2002**, *45*, 5628–5639.
- (44) Nagaoka, Y.; Maeda, T.; Kawai, Y.; Nakashima, D.; Oikawa, T.; Shimoke, K.; Ikeuchi, T.; Kuwajima, H.; Uesato, S. Synthesis and cancer antiproliferative activity of new histone deacetylase inhibitors: Hydrophilic hydroxamates and 2-aminobenzamide-containing derivatives. *Eur. J. Med. Chem.* **2006**, *41*, 697–708.
- (45) These references explain the impact of the high concentration of carbonic anhydrase on the pharmacokinetics of a zinc binding drug. (a) Shank, R. P.; Doose, D. R.; Streeter, A. J.; Bialer, M. Plasma and whole blood pharmacokinetics of topiramate: The role of carbonic anhydrase. *Epilepsy Res.* **2005**, *63* (2–3), 103–112. (b) Martens-Lobenhoffer, J.; Banditt, P. Clinical pharmacokinetics of dorzolamide. *Clin. Pharmacokinet.* **2002**, *41* (3), 197–205.
- (46) Trager, W.; Jensen, J. B. Human malaria parasites in continuous culture. *Science* **1976**, *193*, 673–675.
- (47) Desjardins, R. E.; Canfield, C. J.; Haynes, J. D.; Chulay, J. D. Quantitative assessment of antimalarial activity in vitro by a semiautomated microdilution technique. *Antimicrob. Agents Chemother.* **1979**, *16*, 710–718.

JM061169B